Post-Newtonian orbital evolution and gravitational wave forms of inspiralling compact binaries with mass transfer and spin corrections

Yifan He[1] and Jie Yang[1,2,3,4*]

[1*]School of Physical Science and Technology, Lanzhou University, Lanzhou, 730000, Gansu Province, China.
[2]Institute of Theoretical Physics and Research Center of Gravitation, Lanzhou University, Lanzhou, 730000, Gansu Province, China.
[3]Key Laboratory of Quantum Theory and Applications of MoE, Lanzhou University, Lanzhou, 730000, Gansu Province, China.
[4]Lanzhou Center for Theoretical Physics and Key Laboratory of Theoretical Physics of Gansu Province, Lanzhou University, Lanzhou, 730000, Gansu Province, China.

Contributing authors: heyf21@lzu.edu.cn;

Abstract

In this article, we focus on the effects of mass transfer between binary stars and stellar spin on the post-Newtonian (PN) orbital evolution and gravitational waveforms of compact binary systems. We employ the 2.5PN approximation and the mass quadrupole formula to compute the orbital evolution and gravitational waveforms. After an exhaustive discussion of the astrophysical processes relevant to the scenarios of interest, we summarize a one-dimensional mass transfer model that uniformly treats common envelope evolution and tidal disruption, and derive an approximate expression for the dependence of the mass transfer rate of the material flow through the first Lagrange point L1 on the orbital angular velocity. Furthermore, based on the perturbed Keplerian approach, we present a two-dimensional model for the orbital evolution of compact binary systems that simultaneously accounts for mass transfer and stellar spin corrections. Through numerical simulations, we investigate binary systems with significant relativistic effects, namely NS-NS (neutron star-neutron star), NS-BH (neutron star-black hole), and BH-BH (black hole-black hole) systems, and demonstrate the influence of mass transfer and spin corrections on the orbital evolution and gravitational wave polarization waveforms of these binaries.

Keywords: gravitational waves, Post-Newtonian method, mass transfer, common envelope evolution, tidal disruption, accretion discs

1 Introduction

Gravitational waves were first predicted in 1916 by Albert Einstein himself, the founder of general relativity. Subsequently, considerable debate arose regarding whether gravitational waves possessed physical significance and could be directly observed [1]. In 1975, Taylor and Hulse indirectly confirmed the existence of gravitational waves through observations of the changing period of the PSR1913+16 pulsar binary system [2]. It was not until 2015, when LIGO and Virgo simultaneously and directly detected a gravitational wave signal, GW150914, that the existence of gravitational waves was conclusively established. Since gravitational waves were directly observed by LIGO, humanity has ushered in a new era of gravitational wave astronomy and gravitational wave cosmology.

Gravitational waves provide humanity with an entirely new window to observe the universe, offering a novel class of observational signals beyond electromagnetic (EM) radiation, neutrinos, and cosmic rays, thereby giving rise to the field of multi-messenger astronomy [3]. The first generation of detectors, such as LIGO [4, 5] and Virgo [6, 7], as well as the second generation, including Advanced LIGO [8], Advanced Virgo [9], and GEO-HF [10], and even the third generation, exemplified by the Einstein Telescope Project[11], all hold promise for uncovering more about the universe through gravitational waves (GWs) with increasingly high sensitivity. The sources of gravitational waves can be broadly classified into two categories: those of cosmological origin and those of relativistic astrophysical origin[12]. The former are associated with gravitational waves related to the early universe and cosmic evolution, while the latter primarily focus on gravitational waves emitted by astrophysical processes in the universe, such as the evolution and mergers of compact binaries (primarily neutron stars, white dwarfs, and black holes), supernova explosions, and gravitational waves emitted by the asymmetric rotation of neutron stars, among others.

In the context of General Relativity, gravitational waves exhibit two polarization modes: plus polarization and cross polarization. Experimentally and in data processing, one can decompose gravitational waves into these two polarization modes to study their waveforms, thereby interpreting the cosmic information carried by gravitational waves. In addition to the useful information conveyed by gravitational wave waveforms, we observe that the numerous binary star systems in the Milky Way pose a significant background noise challenge for gravitational wave data processing[13, 14]. Consequently, it is also of great importance to theoretically provide precise gravitational wave template banks for data processing in the detection of extragalactic gravitational waves[15].

For gravitational waves of relativistic astrophysical origin, compact binary systems represent one of the significant sources. To theoretically provide waveform templates for gravitational waves emitted during the evolution of compact binaries, it is first necessary to derive their orbital evolution. Currently, research on the dynamics of

compact binaries primarily employs three methodologies: numerical relativity, post-Newtonian approximation, and black hole perturbation theory. Within the scope of this paper, we primarily adopt the post-Newtonian approximation to study compact binary systems.

The post-Newtonian approximation[16–18] is a systematic approximation to Einstein's field equations under the conditions of low velocities and weak fields, which are typically met in the orbits of most binary systems. Based on approximate methods for the system and combined with harmonic gauge conditions, the post-Newtonian metric can be derived from the energy-momentum tensor of the matter source. Using this metric, equations of motion can be derived from geodesic equations[19], and the propagation of gravitational waves in curved spacetime and their observed waveforms can be studied by considering the post-Newtonian metric field as the spacetime background[18]. For compact binary systems, increasingly precise equations of motion have been obtained [16–18, 20–24]. Regarding post-Newtonian gravitational waves, there are two main research approaches: the Blanchet-Damour approach and the Will-Wiseman approach[25]. The post-Newtonian metric consists of a series of alternating odd and even expansion terms, where it has been found that even-order terms correspond to conserved quantities, while odd-order terms correspond to radiation-reaction (RR) caused by gravitational waves. The RR of gravitational radiation first manifests at the 2.5 post-Newtonian (PN) order, which can be utilized to explain the periodic variation observed in the renowned Hulse-Taylor binary system[2], historically serving as indirect evidence for the existence of gravitational waves. Compact binary systems typically include black hole-black hole (BH-BH), black hole-neutron star (BH-NS), neutron star-neutron star (NS-NS), neutron star-white dwarf (NS-WD), and white dwarf-white dwarf (WD-WD) systems[26]. Building upon the series of work by Blanchet et al.[16], Tagoshi et al. developed post-Newtonian equations of motion that account for spin, still treating the celestial bodies as point masses but now with spin[27], a common property of real celestial bodies, especially neutron stars, which have particularly large spins. Observed neutron star spin frequencies vary from 0.01Hz to 700Hz[28]. Therefore, considering the spin of compact binaries is important.

Unlike the point-mass model, compact binary star systems often possess complex compositional structures. The evolution of these binary systems is influenced by a variety of astrophysical processes, including magnetic interactions[29, 30] (such as magnetic dipole radiation and magnetic reconnection[31, 32]), tidal disruption[33–36](usually occurs in systems with black holes), Roche lobe overflow[37–39], common envelope evolution[40–42], accretion processes[43, 44], radiation pressure[45, 46], and even violent events like various types of supernova explosions[47–50]. Therefore, relying solely on the aforementioned point-mass model to study the evolution of compact binary star systems is inadequate. In our article, we further delve into the impact of mass transfer processes on the evolution of binary stars.

Mass transfer (MT) between two stars in a binary system is a ubiquitous phenomenon in stellar astrophysics, governing the evolution of massive stars [51–53]. For binary systems, the French mathematician Roche proposed the renowned Roche potential, along with derivative concepts such as Roche lobes, Roche radii, and Roche limits, which have become the most prevalent theoretical foundation for discussing

mass transfer today[51]. The Roche potential is an eight-shaped potential field composed of the gravitational forces generated by two compact stars (regarded as point masses) and the inertial centrifugal force. In this potential field, asymmetries arising from differences in mass, density, internal structure, and composition of the two stars often trigger the mass transfer process between them, where one star (typically the less dense one) becomes the donor star, losing mass and transferring it through mass streams to the other star (the primary star or accretor) or its surroundings. Generally, mass transfer mechanisms in compact binary systems are categorized into two types: common envelope evolution and tidal disruption-accretion processes[13]. These processes significantly influence the evolution of binary stars. For instance, mass transfer directly alters the orbital momentum, angular momentum, and energy, impacting the trajectory of the binary stars and thus the waveform of the gravitational waves they emit[13, 54–56]. Mass transfer strips away the outer layers of the donor star, exposing its core, which may initiate violent thermonuclear reactions. For example, a massive main-sequence star undergoing common envelope evolution may expose its stellar core, leading to a supernova explosion and the formation of a neutron star[57]. During the process of mass accretion onto the primary star, radiation pressure can result in the emission of radiation such as X-rays[58], and the accretion process may be accompanied by the formation of an accretion disk due to the combined effects of factors such as the Eddington limit, Magnetic effect, friction, viscosity(mainly caused by turbulence, which may result from magneto-rotational instability[59, 60]), gravitational forces etc.[61, 62]. In summary, since its proposal in 1941, the concept of mass transfer has explained numerous astrophysical phenomena, such as the Algol paradox in detached eclipsing binaries [63–65], X-ray binaries [59, 66–69], cataclysmic variable stars [70**?** , 71], or Type Ia supernovae [47, 48, 50]. In the era of gravitational wave astronomy, MT is crucial for interpreting the mergers of gravitational wave signals from detached binaries. The formation bands of these two MT types are shaped through stable MT or common envelope evolution.

The theoretical analysis and numerical simulations presented in this paper are organized into the following sections. In Section 2, we briefly derive the 2.5 PN metric applicable to general fluid systems, and further consider the energy-momentum tensors for both non-spinning and spinning cases. By combining these with the geodesic equations, we ultimately derive the 2.5 PN equations of motion. In Section 3, we discuss the process of mass transfer, introducing common envelope evolution, tidal disruption-accretion processes, and accretion disks. We then derive the potential impact of mass transfer on the binary orbit. In Section 4, we present the physical properties of white dwarfs and neutron stars, providing examples for later consideration of specific mass transfer scenarios. In Section 5, we introduce the concept of perturbed Keplerian problems and ultimately obtain a model that can account for the evolution of compact binaries with both spin and mass transfer. We also calculate the gravitational waveform observed on Earth using the quadrupole formula. Finally, we employ MATLAB software and utilize the Runge-Kutta method to numerically simulate the results we have obtained and discuss our findings. Throughout this paper, all calculations are in natural units where $G = c = 1$, and the metric signature is $(-,+,+,+)$. The Greek

alpha-beta indices $(\mu, \nu, \alpha, \beta, \dots)$ range over spacetime indices$(0, 1, 2, 3)$. The Latin alphabet indices $(i, j, k, \dots)$ range over only spatial indices$(1, 2, 3)$.

2 Two polarization modes of gravitational waves

For simplicity, we discuss the polarization modes of gravitational waves in flat spacetime[72]. The Einstein tensor $G_{\mu\nu}$ and the stress-energy tensor $T_{\mu\nu}$ are both symmetric tensors of rank $(0, 2)$, each having ten components. Consequently, Einstein's field equations are

$$G_{\mu\nu} = \frac{8\pi G}{c^4} T_{\mu\nu}. \tag{1}$$

which consists of ten equations. They are differential equations involving the metric tensor $g_{\mu\nu}$ and its first and second partial derivatives. Due to the Bianchi identities $\nabla_\nu G_{\mu\nu} = 0$ and the conservation of the stress-energy tensor $\nabla_\nu T_{\mu\nu} = 0$, four of these ten equations are identities, reducing the constraints imposed by the equations on the metric to six. Due to the arbitrariness of coordinate transformations, four of these six constraints are determined by coordinate conditions, leaving only two degrees of freedom with actual physical significance. Under weak-filed approximation, subject the mertic $g_{\mu\nu}$ to a linear decomposition, i.e., letting

$$g_{\mu\nu} = \eta_{\mu\nu} + \hat{h}_{\mu\nu}, \tag{2}$$

where $\eta_{\mu\nu}$ represents the Minkowski metric of flat spacetime, given by $\eta_{\mu\nu} = diag(-1, 1, 1, 1)$, and $\hat{h}_{\mu\nu}$ denotes the perturbation to this flat spacetime, with the superscript indicating the perturbation in flat spacetime to distinguish it from the perturbation in curved spacetime discussed in section 3. We employ the harmonic gauge condition $\partial_\nu g_{\mu\nu} = 0$ along with the Transverse-Traceless (TT) gauge, which means[73]

$$h_{ij}^{TT} = h_{ji}^{TT}, \quad \sum_i h_{ii}^{TT} = 0, \quad \sum_i \nabla_i h_{ij}^{TT} = 0. \tag{3}$$

At this point, Einstein's field equations reduce to

$$\Box \tilde{h}_{\mu\nu} = -\frac{16\pi G}{c^4} T_{\mu\nu}, \tag{4}$$

where $\Box$ is the d'Alembert operator in flat spacetime, given by $\Box = \frac{\partial^2}{\partial t^2} - \nabla^2$, and $\tilde{h}_{\mu\nu} \equiv \hat{h}_{\mu\nu} - \frac{\hat{h}}{2}\eta_{\mu\nu}$, where $\hat{h}$ is the contraction of $\hat{h}_{\mu\nu}$. Let the gravitational wave propagate along the z-axis. In the TT gauge, the non-zero components of $\hat{h}_{\mu\nu}$ are only the spatial components $\hat{h}_{ij}$, which satisfy

$$\hat{h}_{ij} = \hat{h}_{ij}^{TT}. \tag{5}$$

The tensor $\hat{h}_{ij}^{TT}$ can be decomposed into two independent polarization modes: h_+ and $h_\times$. Specifically, it takes the form

$$\hat{h}_{ij}^{TT} = \begin{pmatrix} \hat{h}_+ & \hat{h}_\times & 0 \\ \hat{h}_\times & -\hat{h}_+ & 0 \\ 0 & 0 & 0 \end{pmatrix} \tag{6}$$

Based on the above discussion, we can derive the expressions for the two polarization modes, $\hat{h}_+(t)$ and $\hat{h}_\times(t)$, by calculating the perturbations of spacetime.

3 Post-Newtonian evolution of compact binary systems

3.1 2.5 PN metric for general fluid systems

Under harmonic gauge conditions, Blanchet et,al. employed the post-Newtonian approach to derive the 2.5PN metric of a general fluid system, namely, an arbitrary matter distribution described by an arbitrary stress-energy tensor field $T^{\mu\nu}(\vec{x}, t)$. We employ the following harmonic gauge conditions:

$$\partial_\beta \left[\sqrt{-g} g^{\alpha\beta}\right] = 0, \tag{7}$$

and introduce the Gothic metric

$$\mathfrak{g}^{\alpha\beta} \equiv \sqrt{-g} g^{\alpha\beta}, \tag{8}$$

consequently, the harmonic gauge conditions transform into

$$\partial_\beta \mathfrak{g}^{\alpha\beta} = 0. \tag{9}$$

Define

$$H^{\alpha\mu\beta\nu} \equiv g^{\alpha\beta} g^{\mu\nu} - g^{\alpha\nu} g^{\beta\mu}, \tag{10}$$

at this point, there exists a mathematical identity which states that

$$\partial_{\mu\nu} H^{\alpha\mu\beta\nu} = 2(-g) G^{\alpha\beta} + \frac{16\pi G}{c^4} (-g) t_{LL}^{\alpha\beta}, \tag{11}$$

where $(-g) t_{LL}^{\alpha\beta}$ is the Landau-Lifshitz pseudotensor:

$$
\begin{aligned}
(-g)\, t_{LL}^{\alpha\beta} \equiv \frac{c^4}{16\pi G}\Big[& \partial_\lambda g^{\alpha\beta}\partial_\mu g^{\lambda\mu} - \partial_\lambda g^{\alpha\lambda}\partial_\mu g^{\beta\mu} \\
& + \frac{1}{2} g^{\alpha\beta} g_{\lambda\mu}\partial_\rho g^{\lambda\nu}\partial_\nu g^{\mu\rho} - g^{\alpha\lambda} g_{\mu\nu}\partial_\rho g^{\beta\nu}\partial_\lambda g^{\mu\rho} \\
& - g^{\beta\lambda} g_{\mu\nu}\partial_\rho g^{\alpha\nu}\partial_\lambda g^{\mu\rho} + g_{\lambda\mu} g^{\nu\rho}\partial_\nu g^{\alpha\lambda}\partial_\rho g^{\beta\mu} \\
& + \frac{1}{8}\left(2g^{\alpha\lambda}g^{\beta\mu} - g^{\alpha\beta}g^{\lambda\mu}\right)\left(2g_{\nu\rho}g_{\sigma\tau} - g_{\rho\sigma}g_{\nu\tau}\right)\partial_\lambda g^{\nu\tau}\partial_\mu g^{\rho\sigma}\Big]
\end{aligned}
\tag{12}
$$

The contravariant form of Einstein's field equations is

$$
G^{\alpha\beta} = \frac{8\pi G}{c^4} T^{\alpha\beta} \tag{13}
$$

By substituting eqs. (8) to (11) into eq. (12), and utilizing the condition $\partial_{\beta\mu\nu} H^{\alpha\mu\beta\nu} = 0$, we can derive the following:

$$
\partial_\beta \left[(-g) \left(T^{\alpha\beta} + t_{LL}^{\alpha\beta} \right) \right] = 0 \tag{14}
$$

Define

$$
h^{\alpha\beta} \equiv -\eta^{\alpha\beta} + \mathfrak{g}^{\alpha\beta}. \tag{15}
$$

We can know from eqs. (9) and (10) that

$$
\partial_\beta h^{\alpha\beta} = 0 \tag{16}
$$

By performing variable substitutions using eqs. (8) to (16), one can ultimately obtain the relaxed Einstein equation:

$$
\Box h^{\alpha\beta} = \frac{16\pi G}{c^4} \tau^{\alpha\beta}, \tag{17}
$$

where $\Box = \eta^{\mu\nu}\partial_{\mu\nu}$,$\tau^{\alpha\beta} = (-g)(T^{\alpha\beta} + t_{LL}^{\alpha\beta} + t_H^{\alpha\beta})$, $(-g)\, t_H^{\alpha\beta} = \frac{c^4}{16\pi G}(\partial_\mu h^{\alpha\nu}\partial_\nu h^{\beta\mu} - h^{\mu\nu}\partial_{\mu\nu}h^{\alpha\beta})$. Define

$$
\Lambda^{\alpha\beta}(h) = \frac{16\pi G}{c^4}(-g)\left(t_{LL}^{\alpha\beta} + t_H^{\alpha\beta} \right), \tag{18}
$$

and thus get

$$
h^{\alpha\beta} = \frac{16\pi G}{c^4} |g|\, T^{\alpha\beta} + \Lambda^{\alpha\beta}(h) \tag{19}
$$

which contains the terms at least quadratic in h and/or its derivatives. The relaxed Einstein equation eq. (17), in conjunction with eq. (16), is equivalent to the Einstein field equation eq. (13)[18]. We introduce some notations for specific combinations of certain stress-energy tensors:

$$
\sigma \equiv \frac{T^{00} + T^{ii}}{c^2} \tag{20}
$$

$$\sigma_i \equiv \frac{T^{0i}}{c}, \tag{21}$$

$$\sigma_{ij} \equiv T^{ij}. \tag{22}$$

Then, we introduce some retarded integrals in the following form:

$$V(\vec{x},t) = \Box_R^{-1}\{-4\pi G\sigma\} \equiv G\int \frac{d^3\vec{z}}{|\vec{x}-\vec{z}|}\sigma\left(\vec{z}, t-\frac{|\vec{x}-\vec{z}|}{c}\right), \tag{23}$$

$$V_i(\vec{x},t) = \Box_R^{-1}\{-4\pi G\sigma_i\} \tag{24}$$

$$\hat{W}_{ij} = \Box_R^{-1}\{-4\pi G(\sigma_{ij}-\delta_{ij}\sigma_{kk}) - \partial_i V\partial_j V\} \tag{25}$$

$$\hat{R}_i = \Box_R^{-1}\left\{-4\pi G(V\sigma_i - V_i\sigma) - 2\partial_k V\partial_i V_k - \frac{3}{2}\partial_t V\partial_i V\right\} \tag{26}$$

$$\hat{X} = \Box_R^{-1}\left\{-4\pi GV\sigma_{ii} + 2V_i\partial_t\partial_i V + V\partial_t^2 V + \frac{3}{2}(\partial_t V)^2 - 2\partial_i V_j\partial_j V_i + \hat{W}_{ij}\partial_{ij}^2 V\right\} \tag{27}$$

To obtain the metric at the 2.5 PN order, we utilize the metric at the 1PN order

$$h^{00} = -\frac{4}{c^2}V - \frac{2}{c^4}\left(\hat{W}_{kk} + 4V^2\right) + \mathcal{O}(6) \tag{28}$$

$$h^{0i} = -\frac{4}{c^3}V_i + \mathcal{O}(5) \tag{29}$$

$$h^{ij} = -\frac{4}{c^4}\left[\hat{W}_{ij} - \frac{1}{2}\delta_{ij}\hat{W}_{kk}\right] + \mathcal{O}(6) \tag{30}$$

Substitute eqs. (28) to (30) into the right-hand side of the field equation eq. (17) as an iterative procedure. Meanwhile, use the notations eqs. (23) to (27) to simplyfy expressions. Finally, we obtain the post-Newtonian metric for a general fluid at the 2.5 PN order[19]:

$$g_{00} = -1 + \frac{2}{c^2}V - \frac{2}{c^4}V^2 + \frac{8}{c^6}\left[\hat{X} + V_iV_i + \frac{V^3}{6}\right] + \mathcal{O}(8) \tag{31}$$

$$g_{0i} = -\frac{4}{c^3}V_i - \frac{8}{c^5}\hat{R}_i + \mathcal{O}(7) \tag{32}$$

$$g_{ij} = \delta_{ij}\left(1 + \frac{2}{c^2}V + \frac{2}{c^4}V^2\right) + \frac{4}{c^4}\hat{W}_{ij} + O(6) \tag{33}$$

It is important to note that the post-Newtonian metric field is theoretically valid throughout the entire spacetime[18]. However, in practical applications, it is often valid only in the near zone where the scale is much smaller than the gravitational wavelength, and where retardation effects can be neglected. Under these conditions, the D'Alembert operator approximates to the Poisson operator, i.e., the propagation of gravitational interactions can be considered as instantaneous[25].

3.2 Dynamics of non-spinning compact binary systems

We regard compact binary star systems as composed of two point particles interacting through gravitational forces, described by the following stress-energy tensor:

$$T^{\mu\nu}\left(\vec{x},t\right)=\mu_1\left(t\right)v_1^{\mu}v_1^{\nu}\delta\left(\vec{x}-\vec{y}_1\left(t\right)\right)+1\leftrightarrow 2 \tag{34}$$

Replace the stress-energy tensor in section 3.1 with the form given in eq. (34), and eliminate the divergences caused by the δ-potential through Hadamard regularization[74, 75]. Ultimately, this leads to the post-Newtonian metric field for such compact binary star systems. From the corresponding geodesic equations of the post-Newtonian metric field, we obtain the equations of motion for the reduced mass of the compact binary star system in the center-of-mass frame at the 2.5PN order (during the derivation process, the "order-reduced" technique is adopted to simplify expressions, i.e., replacing the 2.5PN acceleration terms with expressions involving velocity and coordinates using the 1.5PN expressions). We denote the mass of the primary star as m_p, the mass of the companion star as m_c, and the total mass of the binary system as $M=m_p+m_c$, denote $\mu=m_pm_c/M$, $\nu=m_pm_c/M^2$, $q=m_c/m_p$. We denote the relative coordinate vector and velocity vector as $\boldsymbol{x}$ and $\boldsymbol{v}=\mathrm{d}\boldsymbol{x}/\mathrm{d}t$ respectively, defining $\boldsymbol{n}=\boldsymbol{x}/r$ where r is the distance between two stars, and $\dot{r}\equiv\boldsymbol{n}\cdot\boldsymbol{v}$. Finally, we obtain the equations of motion for a non-spinning compact binary star system at the 2.5PN order under the point-mass model:

$$\frac{\mathrm{d}\boldsymbol{v}}{\mathrm{d}t}=-\frac{GM}{r^2}[(1+\mathcal{A})\boldsymbol{n}+\mathcal{B}\boldsymbol{v}]+\mathcal{O}\left(6\right), \tag{35}$$

where the coefficients $\mathcal{A}$ and $\mathcal{B}$ are

$$\begin{aligned}\mathcal{A}=&\frac{1}{c^2}\left\{-\frac{3\dot{r}^2\nu}{2}+v^2+3\nu v-\frac{GM}{r}(4+2\nu)\right\}\\&+\frac{1}{c^4}\left\{\frac{15\dot{r}^4\nu}{8}-\frac{45\dot{r}^4\nu}{8}-\frac{9\dot{r}^2\nu v^2}{2}+6\dot{r}^2\nu^2v^2+3\nu v^4-4\nu^2v^4\right.\\&\left.+\frac{GM}{r}\left(-2\dot{r}^2-25\dot{r}^2\nu-2\dot{r}^2\nu^2-\frac{13\nu v^2}{2}+2\nu^2v^2\right)+\frac{G^2M^2}{r^2}\left(9+\frac{87\nu}{4}\right)\right\}\\&+\frac{1}{c^5}\left\{-\frac{GM}{r}\frac{24\dot{r}\nu v^2}{5}-\frac{G^2M^2}{r^2}\frac{136\dot{r}\nu}{15}\right\},\end{aligned} \tag{36}$$

$$\begin{aligned}\mathcal{B}=&\frac{1}{c^2}\left\{-4\dot{r}+2\dot{r}\nu\right\}\\&+\frac{1}{c^4}\left\{\frac{9\dot{r}^3\nu}{2}+3\dot{r}^3\nu^2-\frac{15\dot{r}\nu v^2}{2}-2\dot{r}\nu^2v^2+\frac{GM}{r}\left(2\dot{r}+\frac{41\dot{r}\nu}{2}+4\dot{r}\nu^2\right)\right\}\\&+\frac{1}{c^5}\left\{\frac{GM}{r}\frac{8\nu v^2}{5}+\frac{G^2M^2}{r^2}\frac{24\nu}{5}\right\}.\end{aligned} \tag{37}$$

3.3 Dynamics of spinning compact binary systems

Many early authors have calculated the gravitational waves emitted by spinning bodies[76–79], including considerations of spin-orbit coupling and spin-spin interactions. However, the spin effects in these works could only be computed up to the 1PN order due to the extreme difficulty in handling the stress-energy tensor with spin. In order to generalize to higher orders (2.5PN), we can adopt the formalism presented in section 3.1 and section 3.2 by treating the stars as point particles (i.e., having a stress-energy tensor with some kind of δ-potential), using Hadamard regularization to eliminate divergences, and then deriving the equations of motion from the post-Newtonian metric field[27]. The stress-energy tensor for a spinning point particle is given by

$$T^{\alpha\beta} = T^{\alpha\beta}_{(M)} + T^{\alpha\beta}_{(S)} + T^{\alpha\beta}_{(SA)}, \tag{38}$$

where

$$T^{\alpha\beta}_{(M)}\left(\vec{x}\right) = \int d\tau p^{\alpha}\left(\tau\right) u^{\beta}\left(\tau\right) \frac{\delta^{(4)}\left(\vec{x} - \vec{y}\left(\tau\right)\right)}{\sqrt{-g}}, \tag{39}$$

$$T^{\alpha\beta}_{(S)}\left(\vec{x}\right) = -\nabla_{\gamma} \int d\tau \hat{S}^{\gamma(\alpha}\left(\tau\right) u^{\beta)}\left(\tau\right) \frac{\delta^{(4)}\left(\vec{x} - \vec{y}\left(\tau\right)\right)}{\sqrt{-g}}, \tag{40}$$

$$T^{\alpha\beta}_{(SA)}\left(\vec{x}\right) = -\frac{1}{2}\nabla_{\gamma} \int d\tau \hat{S}^{\alpha\beta}\left(\tau\right) u^{\gamma}\left(\tau\right) \frac{\delta^{(4)}\left(\vec{x} - \vec{y}\left(\tau\right)\right)}{\sqrt{-g}}, \tag{41}$$

where $u^{\alpha}(\tau)$ represents the 4-velocity of the particle, and p_{ν} represents the 4-momentum of the particle. We use the condition

$$\hat{S}^{\mu\nu} p_{\nu} = 0 \tag{42}$$

to fix the artificial degrees of freedom introduced by treating a spinning compact star as a point particle[80]. Similarly to the processing procedures outlined in section 3.1 and section 3.2, we can derive the 2.5 PN equations of motion for compact binary systems with spin effects. These equations can be expressed as

$$\boldsymbol{a} = \boldsymbol{a}_N + \boldsymbol{a}_{PN} + \boldsymbol{a}_{SO} + \boldsymbol{a}_{SS} + \boldsymbol{a}_{PNSO} + \mathcal{O}\left(6, 8\right), \tag{43}$$

where $\boldsymbol{a}_N, \boldsymbol{a}_{PN}, \boldsymbol{a}_{SO}, \boldsymbol{a}_{SS}, \boldsymbol{a}_{PNSO}$ represent the Newtonian acceleration, the 1PN acceleration, the 1.5PN spin-orbit acceleration, the 2PN spin-spin acceleration, and the 2.5PN spin-orbit acceleration, respectively.

4 Mass transfer between binary stars

4.1 Mass transfer and its one-dimensional model

Due to the density difference between the two stars in a binary system, when the relative distance decreases to a certain scale, the less dense star (the companion) can be torn apart by the other more dense and uniform star (the primary). The process by which the mass of the companion is transferred to the primary or orbits around it is known as the mass transfer process in binary systems. Generally speaking, mass

transfer is mainly classified into two categories: common envelope evolution and tidal disruption-accretion process. In this subsection, we first discuss these two main modes of mass transfer in a general sense and then summarize a general one-dimensional model.

For all discussions about mass transfer in this paper, we adopt the following coordinate system: We assume that the orbital plane is the $xy-plane$ and the centers of the two stars lie on the $x-axis$. The donor star has $x<0$, the accretor has $x>0$, and the first Lagrangian point L_1 is located at the center of the coordinate system, with $x_1=1$.

4.1.1 Common envelope evolution

In the context of common envelope evolution (CE), the outer layers of the companion star (including the photosphere and the denser layers beneath it, or the stellar atmosphere) are gravitationally detached from the companion and form a common envelope that surrounds the binary system on the Roche equipotential surface. A portion of this mass is transferred to the primary star or forms an accretion disk around it through the first Lagrangian point, L1. However, not all the mass is transferred to the primary side through L1. When the mass-loss rate of the companion is high, for instance, if the mass-loss rate of the donor star $\dot{M}_d > 10^{-4} M_{\odot} yr^{-1}$, it is traditionally believed that a significant fraction of the ejected mass is lost to infinity through a rapid, super-Eddington wind[52]. Nevertheless, some researchers, based on an analysis of energy changes and the Roche potential energy, argue that this lost mass is more likely to escape the binary system through the L2 point [81]. For common envelope evolution, several different models have been proposed to address this issue. Traditionally, two distinct models have been introduced based on the physical state of the transferred matter, namely whether the matter is optically thick or optically thin[82–85]. The former treats the matter flow through L1 as a polytropic process, while the latter considers it as an isothermal process. Given the discontinuity between these two approaches based on different physical scenarios, a new unified model has been proposed [52]that transforms the three-dimensional Eulerian hydrodynamic equations of the Roche potential into one-dimensional intrinsic equations through five reasonable assumptions, focusing the mass transfer process on the straight line connecting the two stars.

For an incompressible fluid driven solely by gravitational forces under the Roche potential, and assuming that the mass flow does not radiate nor absorb energy externally, we can derive the hydrodynamic Euler equations governing its behavior in the L_1 region.

$$\frac{\partial \rho}{\partial t} + \nabla \cdot (\rho \boldsymbol{v}) = 0 \tag{44}$$

$$\frac{\partial (\rho \boldsymbol{v})}{\partial t} + \nabla \cdot (\rho \boldsymbol{v} \otimes \boldsymbol{v} + P \boldsymbol{I}) = -\rho \nabla \Phi_R \tag{45}$$

$$\frac{\partial (\rho \epsilon_{tot})}{\partial t} + \nabla \cdot [(\rho \epsilon_{tot} + P) \boldsymbol{v}] = 0 \tag{46}$$

where Φ_R is the Roche potential, $\boldsymbol{v}$ is the three-dementional vector, $\boldsymbol{I}$ is the identity matrix, ϵ_{tot} is the energy per unit mass:

$$\epsilon_{tot} = \epsilon + \frac{1}{2}\boldsymbol{v}^2 + \Phi_R \tag{47}$$

which contains internal energy, kinetic energy, and gravitational potential energy.

We introduce the following five assumptions[52]:

1. The mass flow is stable, i.e. $\partial/\partial t = 0$.
2. The $x-component$ of the velocity does not depend on its position in the $yz-plane$, i.e. $v_x\left(x,y,z\right) = v_x(x)$.
3. The mass flow mainly flows along the $x-axis$, i.e. $v_y^2 \ll v_x^2, v_z^2 \ll v_x^2$, indicating that $\boldsymbol{v}^2 \approx v_x^2$. This assumption also allows us to utilize hydrostatic equilibrium in the $yz-plane$: $\frac{1}{\boldsymbol{\rho}}\nabla P\Big|_{x=const} = -\nabla\Phi_R\Big|_{x=const}$
4. The Roche potential in the vicinity of L_1 can be divided into two parts: one that depends solely on x, denoted as Φ_R^x, and another that depends on both y and z, denoted as Φ_R^{yz}. For Φ_R^{yz}, we use the lowest-order approximation:

$$\Phi_R\left(x,y,z\right) = \Phi_R^x\left(x\right) + \Phi_R^{yz}\left(y,z\right) = \Phi_R^x\left(x\right) + \frac{B}{2}y^2 + \frac{C}{2}z^2 \tag{48}$$

   which directly indicates $\frac{d\Phi_R}{dx} = \frac{d\Phi_R^x}{dx}$
5. The gas exhibits polytropic behavior in the $yz-plane$: $P\Big|_{x=const} = K\rho^{\Gamma}\Big|_{x=const}$, where $K = K\left(x\right)$ and $\Gamma = \Gamma(x)$.

By integrating the aforementioned Euler equations eqs. (44) to (46) on the $yz-plane$, we can ultimately derive the mass transfer rate:

$$\dot{m}_d = v\rho Q_\rho = \frac{2\pi}{\sqrt{BC}}c_T^2 v\rho \tag{49}$$

where c_T is the isothermal sound speed, v is the speed of mass flow and ρ its density, with Q_ρ defined by

$$\rho\left(x\right)Q_\rho = \rho(x,0,0)Q_\rho(x) \equiv \int_{Q(x)} \rho\left(x,y,z\right)dQ, \tag{50}$$

here Q is the so-called effective cross-section at L_1, and $B = (\mathscr{A}-1)\dot{\psi}^2$, $C = \mathscr{A}\dot{\psi}^2$, where $\mathscr{A} = 4 + \frac{4.16}{-0.96+q^{\frac{1}{3}}+q^{-\frac{1}{3}}}$ and $\dot{\psi}$ is the coalescencing angular velocity of the binary orbit[86, 87].

In addition to the aforementioned CE scenario, we can also propose a one-dimensional mass transfer model for the process of tidal disruption and accretion.

4.1.2 Tidal disruption

In the context of tidal disruption-accretion, the distance between compact stars is even closer compared to the scenario of common envelope evolution. The distance from the

companion star's center of mass to the Lagrangian point Ł$_1$ is less than the radius of the companion star, meaning that Ł$_1$ falls within the body of the companion star. At this point, the companion star undergoes tidal disruption, causing a significant amount of matter to escape its self-gravity and form Roche lobe overflow, rapidly flowing towards the primary star. During this process, an accretion disk may form, or the matter may directly flow into the primary star. The proportion of the mass flow entering the accretion disk can be described by a branching coefficient κ, which is primarily related to the mass ratio and, of course, also to the polytropic index of the mass flow[13, 88].

Similar to the previous model calculations of mass overflow in the context of common envelope evolution, we utilize the Euler equations for an ideal incompressible fluid to calculate the mass transfer flow during tidal disruption. Likewise, we compress the mass transfer into the xy-plane and consider the mass overflow from the donor star originating at the point closest to the accretor. Such a model can be considered stable.

Based on conservation conditions, we can derive the following two-dimensional equations for an ideal incompressible fluid:

$$\frac{\partial}{\partial t}\begin{pmatrix}\rho\\ \rho v_x\\ \rho v_y\\ \rho\epsilon\end{pmatrix}+\nabla\begin{pmatrix}\rho v_x & \rho v_y\\ \rho v_x^2+P & \rho v_y v_x\\ \rho v_x v_y & \rho v_y^2+P\\ (\rho\epsilon+P)\,v_x & (\rho\epsilon+P)\,v_y\end{pmatrix}=0. \tag{51}$$

The first term in the above equation represents mass conservation, the second and third terms represent momentum conservation in two directions, and the fourth term represents energy conservation. Here, $\frac{\partial\rho}{\partial t}=0$ indicates that the density at that point remains constant, with ϵ denoting the energy per unit volume. We now write the momentum conservation equation for the point nearest to the donor star on the accretor star side as:

$$\rho\frac{\partial}{\partial t}\begin{pmatrix}v_x\\ v_y\end{pmatrix}+\begin{pmatrix}-\rho g_x+\partial_x P & 0\\ 0 & -\rho g_y+\partial_y P\end{pmatrix}=0 \tag{52}$$

where $\boldsymbol{g}$ represents the effective gravitational acceleration:

$$\boldsymbol{g}=\boldsymbol{g}_p+\boldsymbol{g}_c+\boldsymbol{g}_a=\frac{Gm_p}{r_p^3}\boldsymbol{r}_p+\frac{Gm_c}{r_c^3}\boldsymbol{r}_c+\omega_c^2\boldsymbol{r}_p, \tag{53}$$

where $\boldsymbol{r}_p$ and $\boldsymbol{r}_c$ are the position vectors from the companion star and the primary star to the specified point, respectively. $\boldsymbol{g}_a$ is the centrifugal acceleration, and ω_c is the orbital velocity of the companion star. Further, we can utilize the fact that $\boldsymbol{r}_p$ and $\boldsymbol{r}_c$ are antiparallel to further simplify the expression[13]. However, we will not delve into the details of this point here.

The mass loss rate of the companion star is jointly determined by the flow velocity of the matter stream at the overflow point, the location of the overflow point, and the orbital velocity of the binary stars during the overflow. Therefore, Leibniz's rule can

be utilized to formally express the mass loss rate of the companion star $\dot{m}_c$ as:

$$\dot{m}_c = \frac{\partial m_2}{\partial r}\frac{dr}{dt} + \frac{\partial m_2}{\partial \dot{\psi}}\frac{d\dot{\psi}}{dt} + \frac{\partial m_2}{\partial v}\frac{dv}{dt}_c \tag{54}$$

We will assume that the mass transfer can be reduced to a one-dimensional model (the rationality of which will be discussed in detail later). By substituting the equivalent acceleration into the momentum conservation equation and combining it with the previous equation, we can obtain the final expression as:

$$\dot{m}_c = \frac{\partial m_c}{\partial r}\dot{r} + \frac{\partial m_c}{\partial \dot{\psi}}\ddot{\psi} + \frac{\partial m_c}{\partial v}\left(g\left(r\right) - \frac{1}{\rho\left(r\right)}\left|\nabla P\left(r\right)\right|\right) \tag{55}$$

From the above equation, we can intuitively identify the factors that affect the mass transfer rate. The first term is determined by the distance between the binary stars and the radial acceleration. The second term is determined by the angular velocity and angular acceleration of the binary stars' orbit. And the third term is determined by the outflow rate of the fluid.

We have comprehensively considered the mass transfer model by dividing it into two parts: common envelope evolution and tidal disruption, and have summarized a generalized one-dimensional model based on these two scenarios. However, in the case of tidal disruption, eq. (55) does not admit an analytical solution. Nevertheless, the formal expression eq. (55) remains meaningful because, even without an analytical solution, it provides a more detailed structure for us to approximate and simulate the mass transfer mode. It suggests that we should consider the MT rate comprehensively based on the flow velocity of the matter stream at the overflow point, the location of the overflow point, and the orbital velocity of the binary stars during the overflow. Additionally, under stable common envelope evolution, an analytical solution can be obtained for eq. (55).From eq. (49), and recalling that $B = (\mathscr{A} - 1)\dot{\psi}^2$, $C = \mathscr{A}\dot{\psi}^2$, we can obtain:

$$\dot{m}_c = -\frac{2\pi}{\sqrt{\mathscr{A}\left(\mathscr{A}-1\right)}}\frac{1}{\dot{\psi}^2}c_T^2 v\rho \tag{56}$$

From eq. (56), and assuming that the order of differentiation with respect to time and other variables can be exchanged, we can further obtain:

$$\frac{\partial m_c}{\partial r} = 0 \tag{57}$$

$$\frac{\partial m_c}{\partial \dot{\psi}} = \int \frac{4\pi}{\sqrt{\mathscr{A}\left(\mathscr{A}-1\right)}}\frac{1}{\dot{\psi}^3}c_T^2 v\rho dt \tag{58}$$

$$\frac{\partial m_c}{\partial v} = -\int \frac{2\pi}{\sqrt{\mathscr{A}\left(\mathscr{A}-1\right)}}\frac{1}{\dot{\psi}^2}c_T^2 \rho dt \tag{59}$$

By substituting eqs. (57) to (59) into eq. (55), we obtain the analytical expression for $\dot{m}_c$.

4.2 The accretion disk

An accretion disk is a flat structure composed of gas and dust that orbits around a central celestial body (such as a star or a black hole). Within these disks, material flows toward the central body along spiral paths due to gravitational forces and viscosity, transferring angular momentum outward. Viscosity among the material within the accretion disk creates friction and heating within the disk. This force not only aids in the radial movement of material within the disk but also generates radiation through heating the material, thereby releasing gravitational energy. The typical mass of thin accretion disks around compact binary stars is generally between $10^{-5} - 10^{-8} M_{\odot}$, for an NS-WD system, the total mass of the accretion disk formed around the neutron star after the disruption of the white dwarf is approximately around $10^{-2} - 10^{-3} M_{\odot}$[13].

Regarding the mass transfer scenario where material flows from the first Lagrangian point to an accreting star, it generally results in the formation of an accretion disk around the accreting star. This is because, in the absence of an accretion disk, the transferred mass would flow in a narrow stream from the inner Lagrangian point and form a ring around the accreting star. However, this ring would be too small in size, lacking sufficient tidal interaction with the primary star to facilitate mass transfer to it. Consequently, this portion of mass would be ejected[89, 90]. To fully consider mass transfer, it is essential to take into account the presence of an accretion disk.

The mechanism by which accretion disks transfer mass and angular momentum is extremely complex. It is generally believed that viscosity is one of the primary mechanisms for transferring angular momentum in accretion disks. However, viscosity alone is insufficient to fully explain how angular momentum is transferred from the disk material to its surface. Therefore, turbulence-enhanced viscosity is considered a plausible dynamical theory to explain angular momentum redistribution. The viscosity in accretion disks is mainly caused by turbulence, which may originate from the magneto-rotational instability (MRI)[91]. MRI generates small-scale magnetic field perturbations in the accretion disk, which are continuously amplified during the disk's rotation, ultimately leading to turbulence. This turbulence effectively transfers angular momentum, allowing material to flow from the outer edge of the disk towards the center[61, 92–94].

People have introduced a dimensionless parameter, α, to characterize the viscosity in accretion disks. This parameter is well-defined only when the disk is thin[61]. Many physical properties associated with stable thin disks exhibit weak dependence on alpha. The ignorance of the specific physical properties or the strength of the angular momentum transport process leads to the adoption of this alpha-prescription, which offers a simple and widely applicable picture[61, 95]. We encapsulate all mechanisms related to viscosity within the parameter α.

By employing the parameter α, we can delve deeper into the characteristics of accretion disks and the modes of angular momentum transport, considering various specific scenarios. For cases where the primary star is a neutron star, the best observational evidence suggests that we can adopt α values ranging from 0.1 to 0.4, whereas for cataclysmic variable scenarios, α is approximately 0.1[13, 61].

In the coordinate system we have established(see section 4.1), a thin accretion disk (AD) can be considered as compressed onto the xy-plane, treated as a two-dimensional

mass distribution. For the case where the central object is a neutron star, the surface density and radial velocity of the accretion disk can be expressed as[13]

$$\rho_{surf} = A_\rho \alpha^{-\frac{4}{5}} \dot{m}_{AD\to NS}^{\frac{7}{10}} m_{NS}^{\frac{1}{4}} r_{AD}^{-\frac{3}{4}} \zeta^{\frac{14}{5}} \tag{60}$$

$$v_R = A_v \alpha^{\frac{4}{5}} \dot{m}_{AD\to NS}^{\frac{3}{10}} m_{NS}^{-\frac{1}{4}} r_{AD}^{-\frac{1}{4}} \zeta^{-\frac{14}{5}} \tag{61}$$

$$\zeta = \left[1 - \left(\frac{R_{NS}}{r_{AD}}\right)^{\frac{1}{2}}\right]^{\frac{1}{4}} \tag{62}$$

Here, $\dot{m}_{AD\to NS}$ represents the mass accretion rate onto the neutron star due to the accretion disk (alternatively denoted as $\dot{m}_{AD\to P}$, where P stands for the primary star). r_{AD} is the radial variable for the accretion disk, with range $[R_isco, R_AD]$, where R_{isco} is the radius of the innermost stable circular orbit[18], R_{AD} is the outer radius of the accretion disk, and R_{NS} is the radius of the primary neutron star. A_ρ and A_v are constants, which can be obtained through unit conversion methods as $A_\rho = 87.2645$ and $A_v = 0.0016089$. The matter in the accretion disk moves along the corresponding Keplerian orbits to ensure the stability of the disk. Therefore, the tangential velocity v_τ of the matter in the accretion disk is given by $v_\tau = \sqrt{\frac{Gm_{NS}}{r_{AD}}}$. Consequently, the accretion matter transfers to the primary star at a certain rate, resulting in a change rate of the primary star's mass:

$$\dot{m}_{AD\to P} = \left(\frac{m_{AD} A_\rho^{-1} \alpha^{\frac{4}{5}}}{\int d\theta \int m_p^{\frac{1}{4}} r_{AD}^{-\frac{3}{4}} \zeta^{\frac{14}{5}} dr_{AD}}\right)^{\frac{10}{7}} \tag{63}$$

To study orbital evolution using angular momentum conservation, we assume that the total angular momentum of the binary star system, the accretion disk, and the mass transfer stream is a conserved quantity, denoted as $J_{sum} = J + J_{AD} - J_{mt}$. Here, J represents the angular momentum of the binary star system, J_{AD} represents the angular momentum of the accretion disk, and J_{mt} represents the angular momentum of the mass transfer stream. The negative sign is added for consistency with conventional expressions in the literature. The angular momentum of the accretion disk can be obtained by integrating the density and velocity of the disk over the entire space:

$$J_{AD} = 2\pi \alpha^{-\frac{4}{5}} \dot{m}_{AD\to NS}^{\frac{7}{10}} m_{NS}^{\frac{1}{4}} \sqrt{G m_{NS}} \left(\frac{4}{3} r_{AD}^{\frac{3}{4}} - \frac{14}{5} R_{NS}^{\frac{1}{2}} r_{AD}^{\frac{1}{4}}\right)\Bigg|_{R_{isco}}^{R_{AD}} \tag{64}$$

The rate of change of angular momentum of the accretion disk is given by $\dot{J}_{AD} = \frac{J_{AD}}{m_{AD}}(\dot{m}_{AD} - \dot{m}_{AD\to P})$, where m_{AD} is the mass of AD and $\dot{m}_{AD}$ its time derivative. The rate of change of orbital angular momentum of the binary system due to mass transfer is given by $\dot{J}_{mt} = \dot{m}_p \sqrt{G m_p R_h}$ where

$$R_h \equiv a r_h \tag{65}$$

Here, a is the semi-major axis of the orbit, and r_h is a parameter that depends on the mass ratio q. By comparing the results of numerical calculations, it can be expressed as $r_h \approx a[0.0883 + 0.04858logq + 0.11489log^2q - 0.020475log^3q]$ where$0 < q = \frac{m_c}{m_p} \leq 1$[90]

From the conservation of total angular momentum, $\dot{J}_{sum} = \dot{J}_{so}$, we know that the rate of change of the orbital angular momentum of the binary star system is given by:

$$\dot{J} = -\dot{J}_{AD} + \dot{J}_{mt} + \dot{J}_{so}, \tag{66}$$

where $\dot{J}_{so}$ represents the change in angular momentum of the binary star system due to spin-orbit coupling, primarily caused by tidal interactions and magnetic interactions between the binary stars, and satisfies:[56]

$$\dot{J}_{so} = \frac{km_1r_1^2}{\tau_s}(\omega_s - \omega_o) \tag{67}$$

where ω_s is the rotational frequency of the accreting star, ω_o is the orbital angular frequency, and k is a function of the density profile. Here, we assume that the primary star is a polytrope with its index $n \approx 1.5$, thus k is taken as 0.2. The timescale τ_s becomes the synchronization timescale of the binary system, which is a key quantity to measure the strength of spin-orbit coupling. For double degenerate binary stars, we can explicitly give its expression[96, 97]:

$$\tau_{s,tide} = 1.3 \times 10^7 q^2 \left(\frac{a}{r_2}\right)^6 (\frac{\frac{m_2}{M_\odot}}{\frac{L_2}{L_\odot}})^{\frac{5}{7}} yr \tag{68}$$

$$\tau_{s,mag} = 2 \times 10^6 m_1 r_1^{-4} r_2^{-5} a^6 B^{-2} yr \tag{69}$$

Where L_2 represents the luminosity of the companion star, $L_\odot$ represents the luminosity of the Sun, and B represents the surface magnetic field of the accreting star in Gauss. The evolution of the rotational frequency of the accreting star with respect to the orbital angular frequency is described as follows:

$$\dot{\omega}_s = \dot{\omega}_o + \dot{\Omega}_{so} = \lambda\omega_s\frac{\dot{m}_2}{m_1} - \frac{\dot{J}}{km_1r_1^2} - \frac{\Omega_{so}}{\tau_s} \tag{70}$$

where $\Omega_{so} = \omega_s - \omega_o$ and $\lambda = 1 + 2\frac{dlnr_1}{dlnm_1} + \frac{dlnk}{dlnm_1}$.

In order to investigate the mass change rate of the primary star $\dot{m}_p$, we introduce the branching coefficient κ to signify the proportions of mass flow directed towards different pathways. We understand that part of the change in the mass of the primary star, is caused by the accretion disk, specifically denoted as $\dot{m}_{AD\to P}$. Therefore, κ is defined as

$$\kappa = \left[\frac{\delta m_p - \delta m_{AD\to P}}{\delta m_c}\right] \tag{71}$$

which can further be expressed as

$$\kappa\left(\eta_w, \gamma_a\right)=\frac{1-\eta_w \gamma_a+\sqrt{-5{\gamma_a}^2+10 \eta_w {\gamma_a}^2+{\eta_w}^2 {\gamma_a}^2+6 \gamma_a}}{2\left(-\gamma_a+2 \eta_w \gamma_a+1\right)}, \tag{72}$$

among them, γ_a represents the adiabatic index. For stable white dwarfs, γ_a can be taken as 5/3 (for the non-relativistic case with lower density) or 4/3 (for the extreme relativistic case). η_w stands for the wind cooling efficiency, which is a function of the mass ratio and represents the rotational efficiency coefficient. For simplicity and physical feasibility, we can approximately take $\eta_w \approx 110.1093/\mathrm{mnras/stw1410}$. Based on the definition of the branching coefficient, we can express the mass change rate of the primary star as:

$$\dot{m}_p=\kappa(q)\left(-\dot{m}_c\right)+\dot{m}_{AD \rightarrow P} \tag{73}$$

Incorporating the branching coefficient, we can determine that the rate at which the accretion disk obtains mass from the companion star is

$$\begin{aligned}\dot{m}_{C \rightarrow AD}=\left(1-\kappa\left(q\right)\right)\Bigg\{&\frac{2 \pi}{\sqrt{\left(\mathscr{A}-1\right) \mathscr{A}}} \dot{\psi}^{-2} c_T^2 v \rho \\ &+\left[\frac{\partial m_2}{\partial r} \dot{r}+\frac{\partial m_2}{\partial \dot{\psi}} \ddot{\psi}+\frac{\partial m_2}{\partial v}\left(g\left(r\right)-\frac{1}{\rho\left(r\right)}\left|\nabla P\left(r\right)\right|\right)\right]\Bigg\}\end{aligned} \tag{74}$$

Therefore, the mass changing rate of the accretion disk is:

$$\dot{m}_{AD}=\dot{m}_{C \rightarrow AD}-\dot{m}_{AD \rightarrow P} \tag{75}$$

Where $\dot{m}_{C \rightarrow AD}$ and $\dot{m}_{AD \rightarrow P}$ are given by eq. (74) and eq. (63), respectively. Therefore, the mass of the accretion disk at a particular time t is given by the following integral:

$$m_{AD} \equiv M-m_p-m_c=\int_0^t\left(\dot{m}_{C \rightarrow AD}-\dot{m}_{AD \rightarrow P}\right) d t \tag{76}$$

Taking into account common envelope evolution, tidal disruption and accretion, as well as the different sources of mass obtained by the primary star described by κ in the presence of an accretion disk, we can summarize the mass transfer rate of the primary star as

$$\begin{aligned}\dot{m}_p=\kappa\left(q\right)\Bigg\{&\frac{-2 \pi}{\sqrt{\left(\mathscr{A}-1\right) \mathscr{A}}} \dot{\psi}^{-2} c_T^2 v \rho \\ &-\left[\frac{\partial m_2}{\partial r} \dot{r}+\frac{\partial m_2}{\partial \dot{\psi}} \ddot{\psi}+\frac{\partial m_2}{\partial v}\left(g\left(r\right)-\frac{1}{\rho\left(r\right)}\left|\nabla P\left(r\right)\right|\right)\right]\Bigg\}+\dot{m}_{AD \rightarrow P}\end{aligned} \tag{77}$$

From eq. (66), we know that the total change in orbital angular momentum at this time due to the mass flow in the mass transfer process and the presence of the accretion

disk is given by:

$$\dot{J} = -\dot{J}_{AD} + \dot{J}_{mt} + \dot{J}_{so} = -\frac{J_{AD}}{m_{AD}}\left(\dot{m}_{AD} - \dot{m}_{AD\to P}\right) + \dot{m}_p\sqrt{Gm_pR_h} + \dot{J}_{so}, \tag{78}$$

where $\dot{J}_{AD}$, m_{AD}, $\dot{m}_{AD}$, $\dot{m}_{AD\to P}$, $\dot{m}_p$, R_h are given by eq. (64), eq. (76), eq. (75), eq. (63), eq. (77) and eq. (65) respectively. So far, we have fully obtained the specific expressions for the mass changing rate of the primary and companion stars, as well as the evolution of orbital angular momentum of the binary system, under our mass transfer model and accretion disk model.

4.3 Dependence of mass transfer rate on orbital parameters

In order to ultimately derive the impact of mass transfer on the orbital evolution of binary stars and facilitate subsequent numerical simulations, we need to further analyze and obtain a reasonably simplified mass transfer rate (MT rate) as a function of orbital parameters. We can consider the mass transfer stream flowing out of the L_1 region into the orbital region by compressing it onto the two-dimensional $xy-plane$, as hydrostatic equilibrium is often satisfied in the z-direction, making it reasonable to neglect the third dimension[89]. For the MT rate near L_1, we can make an approximate treatment similar to the method used for thin galactic accretion disks. The results indicate that under such a model, the MT rate is proportional to the orbital rotation frequency $\dot{\psi}$.

The MT rate from the donor star passing through L_1 point along the $x-axis$ is

$$\dot{M}_c = -v\rho Q_\rho = -\frac{2\pi}{\sqrt{BC}}c_T^2 v\rho \tag{79}$$

Since the material stream flows along the $x-axis$, from eq. (48) we can deduce that

$$\frac{\partial\Phi_R(x,y,z)}{\partial x} = \frac{\partial\Phi_R^x(x)}{\partial x} \tag{80}$$

i.e., performing a Taylor expansion of $\Phi_R(x,y,z)$ along the $x-axis$ is equivalent to performing a Taylor expansion of the unary function $\Phi_R^x(x)$ with respect to x. We Taylor expand $\Phi_R^x(x)$ at the L_1 point up to the next-to-leading order:

$$\Phi_R^x(x) = \left.\frac{\partial\Phi_R^x(x)}{\partial x}\right|_{L_1} x + \frac{1}{2}\left.\frac{\partial^2\Phi_R^x(x)}{\partial x^2}\right|_{L_1} x^2 \tag{81}$$

By definition, the sum of the gravitational force and the inertial force at a Lagrangian point is zero, therefore the first term in eq. (81) vanishes. Additionally, we have assumed before that $\frac{\partial\rho}{\partial t} = 0$, which indicates that the density distribution is stable. Thus, the density function is not a function of orbital parameters. Consider a particle with a mass of Δm located on the $x-axis$ with an x-coordinate of $x_{\Delta m} = \Delta l$, where

both Δm and Δl are small quantities. Since the resultant force of the gravitational and inertial forces acting on the particle is zero, we have $\frac{\partial \Phi_R^x(0)}{\partial x} = 0$, and

$$\frac{\partial \Phi_R^x(\Delta l)}{\partial x} = \Delta m \Delta l \dot{\psi}^2, \tag{82}$$

$$\frac{\partial^2 \Phi_R^x(x)}{\partial x^2} | L1 = \lim_{\Delta l \to 0} \frac{\frac{\partial \Phi_R^x(\Delta l)}{\partial x} - \frac{\partial \Phi_R^x(0)}{\partial x}}{\Delta l} = \lim_{\Delta l \to 0} \frac{\frac{\partial \Phi_R^x(\Delta l)}{\partial x}}{\Delta l} = \Delta m \dot{\psi}^2 \tag{83}$$

Since $\Delta m = \rho \delta(x)$ and ρ does not undergo an abrupt change near L_1, Δm is a constant value in the vicinity of L_1. Consequently, $\frac{\partial \Phi_R^x(\Delta l)}{\partial x} \propto \dot{\psi}^2$. Substituting the above relationships into eq. (81), we obtain

$$\Phi_R^x(x) \propto \frac{1}{2} \dot{\psi}^2 x^2 \tag{84}$$

Assuming that the mass flow reaches the adiabatic sound speed c_s at the L_1 point. In order for the material to pass through the L_1 region via the effective cross-section, it must overcome the gravitational potential:

$$\Delta \Phi_R^x(x) = \frac{1}{2} \frac{\partial^2 \Phi_R^x(x)}{\partial x^2} \bigg|_{L_1} x^2 - \frac{\partial \Phi_R^x(0)}{\partial x} \propto \frac{1}{2} \dot{\psi}^2 x^2 \tag{85}$$

Typically, the area scale of the effective cross-section is Q_ρ, and it has an angle of 19.5° to 28.4° relative to the line connecting the centers of the two stars[89], so roughly speaking, the scale along the x-axis is on the order of $\sqrt{Q_\rho}$. At this point, we can obtain the adiabatic sound speed c_s near the L_1 point:

$$c_s^2 \approx 2 \Delta \Phi_R^x \left(\sqrt{Q_\rho} \right) \propto \frac{1}{2} \dot{\psi}^2 Q_\rho \tag{86}$$

Recall that we have previously assumed that the mass flow passing through the L_1 point is isothermal and adiabatic along the streamline, and therefore can be described using a polytropic equation of states(EOS)[82]. Thus, we have:

$$c_s^2 = \Gamma c_T^2 \tag{87}$$

where Γ represents the polytropic component. The effect of varying Γ on the MT rate is quite small. For example, for optically thick gas flows, the impact of varying Γ on the MT rate is less than 4%[98]. Therefore, we assume here that Γ is constant, and thus

$$c_s^2 \propto c_T^2 \tag{88}$$

As for eq. (79), we have $v \approx c_s$, then the MT rate $\dot{M}_2 = -\frac{2\pi}{\sqrt{BC}} c_T^2 v \rho \approx -\frac{2\pi}{\sqrt{BC}} c_T^2 c_s \rho = \frac{-2\pi}{\sqrt{(\mathscr{A}-1)\mathscr{A}}} \dot{\psi}^{-2} c_T^2 c_s \rho$. Additionally, considering eq. (86) and eq. (88), we finally arrive

at

$$\dot{M}_2 = -\beta\dot{\psi}, \tag{89}$$

where, the positive coefficient β introduced is determined by factors such as the mass ratio q of the binary stars, the velocity of the mass flow in the L_1 region, the effective temperature of the mass flow, the EOS of the mass flow, and the polytropic coefficient. Consequently, in addition to the impact of the mechanisms inherent to the mass transfer process itself, generally speaking, the influence of the orbital parameters of the binary stars on the mass transfer rate (MT rate) is mainly manifested through an effect with an exponent of 1 on the angular rotational velocity $\dot{\psi}$.

5 Quasi-Keplerian orbital evolution of compact binary systems

In order to ultimately determine the impact of mass transfer on gravitational waveforms of compact binary systems, we must first derive a systematic approach to studying the orbital evolution of it, and the perturbed Keplerian method[1] is used. We aim to utilize this method to integrate the orbital evolution caused by mass transfer between binary stars with the relativistic post-Newtonian effects arising from the spins of compact stars, thereby establishing a general methodology for dealing with realistic compact binary systems that incorporate mass transfer and the relativistic effects including ones caused by the spins of the stars.

It is important to note that the influence of the aforementioned physical processes on orbital evolution occurs at two levels. One is the impact stemming from the mechanisms of mass transfer, including angular momentum transfer due to mass flow, spin-orbit coupling (in the classical context, primarily resulting from dissipative coupling, tides, magnetic fields, etc., such as dissipation induced by currents within the donor star due to the magnetic field of the accreting star in WD-NS systems[96]), additional energy changes caused by thermonuclear reactions, and orbital perturbations caused by supernova explosions and recoil. Additionally, there are relativistic effects due to the significant energy-momentum tensor of compact binary systems, leading to non-negligible spacetime curvature.

The fundamental reason for utilising the perturbed Keplerian method to uniformly address these two aspects is our observation that the existing picture of mass transfer is essentially classical. Thus, all orbital impacts resulting from mass transfer can be fully described using classical dynamical quantities such as momentum, angular momentum, and energy (mathematically represented as low-order tensors), which have direct connections with Keplerian parameters (e.g., the semi-latus rectum of a Keplerian orbit, $p = \frac{L^2}{GM\mu^2}$). Furthermore, post-Newtonian correction terms can be regarded as perturbations expanding from low to high orders of Newtonian gravity, allowing us to still consider the orbit at any given moment as a Keplerian orbit under Newtonian gravity plus corrections due to relativistic effects. The latter are provided by the perturbed Keplerian method, which gives evolution equations for Keplerian orbital parameters, enabling the study of orbital evolution of binary systems in the phase

[1] This approach is generally called the "perturbed Keplerian problem" in the literature, but we treat it as a method here, see [**?**].

space of Keplerian orbits. These ideas are all based on the treatment using the reduced mass $\mu = \frac{m_1 m_2}{m_1+m_2}$.

We denote the longitude of pericenter as ω and the true anomaly as f. To simplify the discussion, we restrict the Keplerian orbit to be two-dimensional, i.e., the binary stars move in the $xy-plane$. We can consider the acceleration as the Newtonian acceleration plus a so-called "perturbing force"[**?**]:

$$\boldsymbol{a} = -\frac{Gm}{r^2}\boldsymbol{n} + \boldsymbol{f}, \tag{90}$$

where

$$\boldsymbol{f} = R\boldsymbol{n} + S\boldsymbol{\lambda} \tag{91}$$

where $\boldsymbol{n}$ and $\boldsymbol{\lambda}$ are the unit vectors in the radial and tangential directions, respectively. By projecting $\boldsymbol{a}$ onto these two directions, expressions for R and S can be obtained. Here, we only consider the acceleration eq. (43) derived previously, which includes post-Newtonian corrections. Using the R and S obtained above, we can derive the influence of post-Newtonian corrections and spin on the rates of change of Keplerian orbital parameters:

$$\dot{p}_{PN} = 2\sqrt{\frac{p^3}{GM}}\frac{1}{1+ecosf}S, \tag{92}$$

$$\dot{e}_{PN} = \sqrt{\frac{p}{GM}}[sinf\ R + \frac{2cosf + e\left(1+cos^2 f\right)}{1+ecosf}S], \tag{93}$$

$$\dot{\omega}_{PN} = \frac{1}{e}\sqrt{\frac{p}{GM}}\left[-cosf\ R + \frac{2+e\ cosf}{1+e\cos f}sinf\ S\right]. \tag{94}$$

Denoting the major semi-axis and eccentricity of the Keplerian orbit as a and e respectively, we have:

$$a = \frac{p}{1-e^2}, \tag{95}$$

$$e = \sqrt{1+\frac{2EL^2}{G^2M^2\mu^2}}. \tag{96}$$

We consider M, μ, E, and L as functions of time, a and e change with time accordingly.

We note that when viewing the motion from the perspective of perturbed Keplerian orbits, the perturbations to the orbit due to post-Newtonian corrections are complex, whereas the perturbations to the orbit caused by mass transfer processes can be fully described using orbital energy and angular momentum, as this process is classical. For the former, however, the orbital perturbations go beyond the description of "energy and angular momentum loss." With this in mind, we project the acceleration equation eq. (43) onto $\boldsymbol{n}$ and $\boldsymbol{\lambda}$ to obtain the values of R and S (see eq. (91)), in order to address their contributions to the evolution of Keplerian parameters.

Next, we calculate the time derivatives of p and e due to mass transfer. Since the Keplerian orbit we consider is two-dimensional, its phase space is also two-dimensional, and thus the trajectory can be fully determined by the two parameters p and e. The energy changes during the mass transfer process are extremely complex, including

processes such as thermonuclear reactions. However, we can macroscopically obtain the dominant rate of energy change:

$$E = \frac{GM}{2}\frac{e^2-1}{p}, \tag{97}$$

$$\dot{E}_{MT} = -\frac{1}{2}[\frac{Gp\left(\dot{M}\mu - M\dot{\mu}\right) - \dot{p}GM\mu}{p^2}(1-e^2)] \tag{98}$$

We can derive the rates of change for p and e as follows:

$$\dot{p}_{MT} = \frac{2L\dot{L}_{MT}}{GM\mu^2} - \frac{L^2\dot{M}_{MT}}{GM^2\mu^2} - \frac{2L^2\dot{\mu}_{MT}}{GM\mu^3}, \tag{99}$$

$$\dot{e}_{MT} = \frac{\left(\frac{2L^2\dot{E}_{MT}}{G^2M^2\mu^2} + \frac{4EL\dot{L}_{MT}}{G^2M^2\mu^2} - \frac{4EL^2\dot{M}_{MT}}{G^2M^3\mu^2} - \frac{4EL^2\dot{\mu}_{MT}}{G^2M^2\mu^3}\right)}{2\sqrt{1+\frac{2EL^2}{G^2M^2\mu^2}}} \tag{100}$$

where $\dot{L}_{MT}$ is the time evolution of the orbital angular momentum of the binary system due to mass transfer (in our mass transfer model, it's just $\dot{J}$ given by eq. (66)), and $\dot{M}_{MT}$ and $\dot{\mu}_{MT}$ are the rates of change of the total mass and reduced mass of the binary system due to mass transfer, specifically:

$$\dot{M}_{MT} = (1-\kappa(q))\,\dot{m}_c + \dot{m}_{AD\to P} \tag{101}$$

$$\dot{\mu}_{MT} = \frac{\dot{m}_p m_c + m_p\dot{m}_c}{M} - \frac{\dot{M}_{MT}m_p m_c}{M^2} \tag{102}$$

The above is the effects of mass transfer on the evolution of binary star systems.

Combining eqs. (92) and (93) with eqs. (99) and (100), we can obtain the final rate of change for the perturbed Keplerian orbital parameters:

$$\dot{p} = \dot{p}_{PN} + \dot{p}_{MT}, \tag{103}$$

$$\dot{e} = \dot{e}_{PN} + \dot{e}_{MT}. \tag{104}$$

To obtain the evolution equation for ω, we introduce two unknown variables, $R^{'}$ and $S^{'}$, which satisfy the following system of equations:

$$\dot{p} = 2\sqrt{\frac{p^3}{GM}}\frac{1}{1+ecosf}S^{'}, \tag{105}$$

$$\dot{e} = \sqrt{\frac{p}{GM}}[sinf\ R^{'} + \frac{2cosf + e\left(1+cos^2f\right)}{1+ecosf}S^{'}]. \tag{106}$$

The $\dot{p}$ and $\dot{e}$ among the above equations are given by eq. (103) and eq. (104) respectively. By solving the above system of equations for $R^{'}$ and $S^{'}$, we can obtain the evolution of the longitude of pericenter ω:

$$\dot{\omega} = \frac{1}{e}\sqrt{\frac{p}{GM}}\left[-cosf\ R^{'} + \frac{2+e\ cosf}{1+e\cos f}sinf\ S^{'}\right], \tag{107}$$

along with

$$\dot{f} = \frac{L}{\mu^2 r},\ r = \frac{p}{1+ecosf}. \tag{108}$$

eq. (103), eq. (104), eq. (107) and eq. (108) comprehensively describe the evolution of orbital parameters. By further integrating these equations using the Runge-Kutta method in numerical simulations, we can ultimately obtain an orbit that takes into account both mass transfer and post-Newtonian corrections (including spin effect). With the knowledge of the orbital evolution of the binary system, and by applying the quadrupole formula, we can further derive the waveforms of the two polarization modes of the gravitational waves emitted by the compact binary systems as observed by an observer.

6 Numerical results

Compact binary systems typically consist of black holes, neutron stars, and white dwarfs[26]. In this paper, we primarily consider compact binary systems composed of neutron stars and black holes to illustrate our results, as such binary systems often possess higher spins and stronger gravitational fields compared to those containing white dwarfs.

Neutron stars generally exhibit strong magnetic fields, typically ranging from $10^{10} \sim 10^{13} Gauss$. For double neutron star systems (NS-NS), we consider factors influencing their orbital evolution to include gravitational interactions (primarily Newtonian gravity, post-Newtonian corrections, and tidal dissipation) as well as magnetic interactions. The timescale for tidal interactions, $\tau_{s,tid}$, depends on the internal structure of the neutron stars, the orbital detachment, and the efficiency of tidal dissipation[56]. Due to the extremely high density within neutron stars, the efficiency of tidal dissipation is very low. For a typical neutron star system with parameters as shown in table 1, we can estimate the tidal interaction timescale to be $\tau_{s,tid} \approx 1.3 \times 10^{19} yr$, while the magnetic interaction timescale to be $\tau_{s,mag} \approx 2.8 \times 10^{-30} yr$. Therefore, tidal interactions can be neglected compared to magnetic interactions. The

Table 1 An example of NS-NS systems

System	m_1 ($M_\odot$)	m_2 ($M_\odot$)	a (m)	r_1 (m)	r_2 (m)	B (G)	L_2[1] ($L_\odot$)	ω_s (Hz)	ω_o (Hz)
NS-NS	1.4	1.4	10^6	10^4	10^4	10^{12}	0.1	100	0.1

[1]The luminosity of the secondary star.

effects of magnetic interactions on orbital evolution[99] are mainly manifested in two aspects: firstly, magnetic dipole radiation[30, 100] (where the magnetic field of a neutron star interacts with its rotational motion, leading to the dissipation of energy and angular momentum through magnetic dipole radiation); secondly, magnetic reconnection (where the magnetic fields of two neutron stars interact, which converts magnetic energy to plasma energy, resulting in changes in their spin angular momentum[101]). The intensity of electromagnetic dissipation also depends on the uncertain resistance in the space between the stars $\mathcal{R}_{space}$. Generally, the smaller the $\mathcal{R}_{space}$, the greater the dissipation. When $\mathcal{R}_{space}$ is small, electric dissipation predominantly occurs in the surface layers of the magnetic NS, and can reach $\sim 10^{49} erg\ s^{-1}$. At this point, when the dipole fields exceed approximately $10^{12}G$, magnetic torques will have a significant impact on the spin of the neutron star[99].

The above results indicate that the influence of magnetic interactions on the evolution of spin angular momentum is extremely significant, suggesting that the spin angular momentum of a neutron star can dissipate rapidly due to magnetic interactions. Therefore, in our numerical simulations, we assume that the binary star system is locked due to magnetic interactions, meaning that the rotational angular velocity is the same as the orbital angular velocity.

Set the initial mass of the primary star as $m_p = 2M_\odot$, the initial mass of the companion star as $m_c = 1.4M_\odot$, the initial eccentricity as $e_0 = 0.4$, the initial periapsis distance for a quasi-Keplerian orbit at ${100M_\odot}^{-1}$, and the initial position at the apoapsis with $\psi = \pi$.

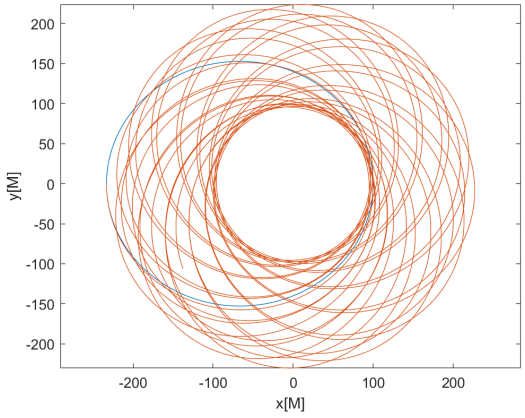

Fig. 1 The blue line represents the trajectory under Newtonian gravity, while the red line represents the motion trajectory with 2.5 PN correction. We can observe that for NS-NS system, the effects of post-Newtonian corrections are extremely significant, making post-Newtonian corrections necessary.

From fig. 1, it can be observed that under Newtonian gravity, the orbit is an elliptical Keplerian orbit. However, for the orbit under 2.5 PN corrections, it initially resembles the elliptical orbit of Newtonian gravity within the first period but gradually

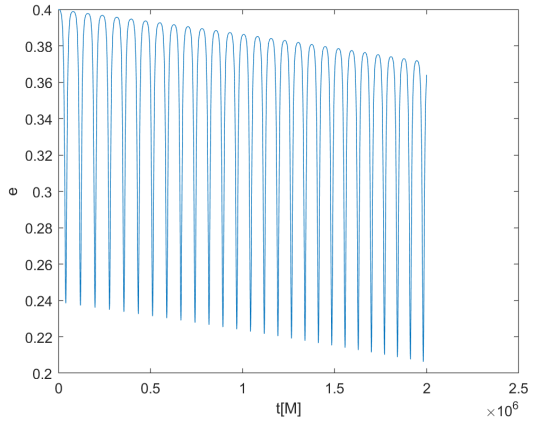

Fig. 2 The upper figure demonstrates the evolution of orbital eccentricity e over time with 2.5 PN correction.

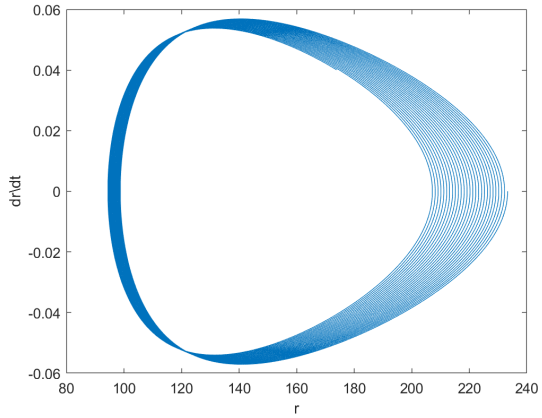

Fig. 3 The upper figure is the phase diagram of r vs $\dot{r}$

exhibits significant precession. We can clearly see that the orbits near the pericenter of each period under post-Newtonian corrections roughly enclose a circle (this point will be further explained in conjunction with fig. 3 later).

fig. 2 depicts the evolution of orbital eccentricity over time under 2.5PN correction. We can observe rapid fluctuations in the eccentricity near the pericenter, with more dramatic orbital changes. After rapidly decreasing to a trough at the pericenter, the eccentricity quickly rebounds, while at the apocenter, the eccentricity changes more smoothly, overall showing a relatively smooth downward trend. This indicates that during the stable inspiral phase, the eccentricity oscillates and decreases slowly, showing a trend of circularization.

fig. 3, with $\dot{r}$ on the vertical axis and r on the horizontal axis, displays the variation of rdot at different r values. On the left side of fig. 3, the region traversed by the

phase trajectory is very narrow horizontally. During the process where $\dot{r}$ decreases to zero and then rises again, the change in r is much smaller than that on the right side, despite the same change in rdot. This suggests that the motion near the pericenter corresponding to the left side of the figure occurs over a much shorter period of time, with a much larger rate of change in $\dot{r}$, and thus a much larger change in eccentricity. Therefore, the definition of the mean eccentricity e fails near the pericenter, leading to sharp valleys in fig. 2 at the pericenter. Conversely, at the apocenter, the eccentricity is lower, and the trajectory evolution is less dramatic. From fig. 2, the eccentricity at the apocenter is relatively smooth and gradually decreases overall, reflecting the gradual circularization of the binary system due to gravitational radiation. Compared to the apocenter, the narrow horizontal range of the phase trajectory near the pericenter indicates small changes in r, which is why the orbit near the pericenter in $figure1$ roughly encloses a circular shape.

Next, we adopt the mass transfer hypothesis given by eq. (89) and employ numerical simulations to investigate the impact of mass transfer on the orbit and waveforms. From fig. 4, we can observe that mass transfer can lead to a relatively significant

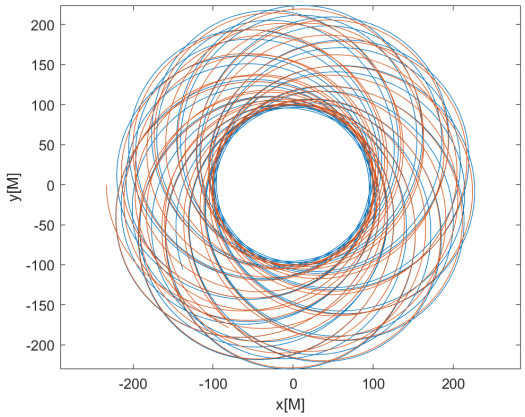

Fig. 4 In the upper figure, the blue line represents the trajectory under 2.5PN correction, while the red line shows the trajectory with mass transfer, where the mass transfer parameter $\beta = 0.0001$.

modification of the orbit. Reflecting on the plus polarized gravitational wave waveform shown in fig. 5, we can deduce that mass transfer accelerates the evolution of the orbiting compact binary star system, causing it to exhibit a phase advancement.

To illustrate the effects of post-Newtonian correction due to spin on orbital evolution, we plot the evolutionary trajectories for three cases: without spin corrections, with the stars spinning at the frequency of orbital angular frequency because of magnetic locking, and with the primary star spinning at a higher frequency of $700Hz$, as shown in fig. 6.

From fig. 6, it can be observed that for the case of NS-NS system, the post-Newtonian effects due to spin are negligible. Considering that neutron stars have

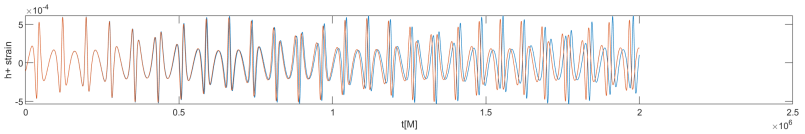

Fig. 5 The figure above displays the plus-polarized gravitational wave waveform corresponding to the post-Newtonian trajectory. The blue line represents the waveform without mass transfer, while the red line represents the waveform with mass transfer, $\beta = 0.0001$. The mass transfer results in an overall phase advancement of the waveform. The large fluctuations in the waveform as a whole are due to the orbital precession.

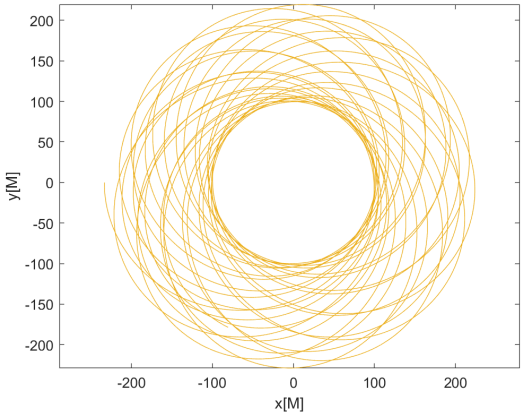

Fig. 6 In the figure above, the blue line represents the trajectory under 2.5PN correction in the case of *tidal&magnetic* locking. The red line would be the trajectory incorporating post-Newtonian effects induced by spin. However, the yellow line, which depicts the trajectory when the neutron star is spinning at a frequency of $700Hz$, is the only one visible in the figure because all three trajectories almost completely overlap. Mass transfer coefficient $\beta = 0.0001$.

significantly higher densities and rotational frequencies compared to white dwarfs, it is reasonable to extrapolate that the post-Newtonian effects of white dwarf rotation can also be ignored. However, black holes typically possess much larger spins. Assuming a binary system consisting of a Kerr black hole with a mass of $3M_{\odot}$ and a spin of $\chi_{BH} = 0.8$, paired with a neutron star of $1.5M_{\odot}$, we set the initial eccentricity to $e_0 = 0.4$, the initial periastron distance of the quasi-Keplerian orbit to $100M_{\odot}^{(} - 1)$, and the initial position at the apoastron with $\psi = \pi$. The resulting trajectory is shown in fig. 7.

From fig. 7, we can see that for rapidly rotating compact celestial bodies, such as those with $\chi_{BH} = 0.8$, the post-Newtonian corrections due to spin have a relatively significant impact on orbital evolution.

Based on the above discussions, we utilize our method to comprehensively consider an NS-BH system, taking into account both mass transfer and spin corrections to the orbit, and investigate the corresponding gravitational wave polarization waveforms.

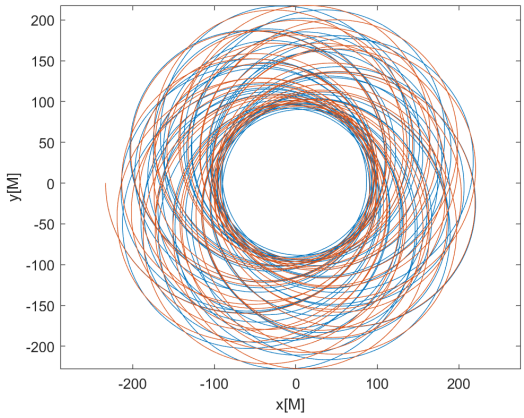

Fig. 7 The above figure demonstrates the trajectories of the NS-BH system, with the blue line representing the case without spin correction and the red line representing the case with spin correction, the spin of the black hole $\chi_{BH} = 0.8$.

Assuming an NS-BH system with mass transfer, and considering the gravity is the dominant interaction, setting parameters consistent with those used in fig. 7, and with the mass transfer process described by eq. (89), the neutron star is accreted by the black hole, with a mass transfer parameter $\beta = 0.0001$.

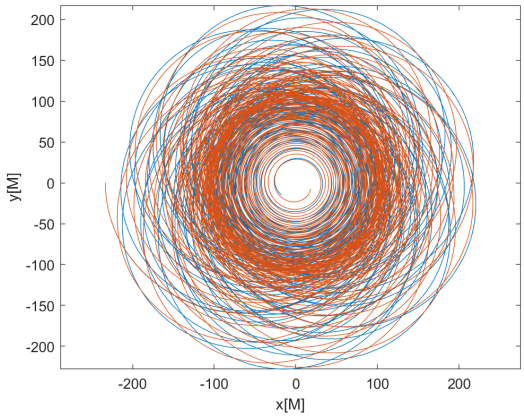

Fig. 8 In the above figure, the blue line represents the trajectory of the NS-BH system, while the red line depicts the trajectory that takes into account both spin and mass transfer corrections. The cutoff condition is set at a velocity greater than $0.4c$, beyond which post-Newtonian methods are deemed no longer applicable.

fig. 9 demonstrates the effects of mass transfer and spin corrections on the gravitational wave waveform. We can notice a change in amplitude at the peak of the wave, which is primarily a characteristic resulting from mass transfer. This is because the

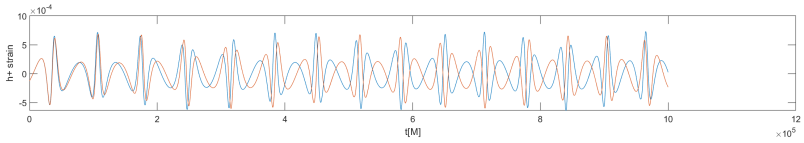

Fig. 9 In the above figure, the blue line represents the trajectory of the NS-BH system, while the red line, which incorporates corrections for both spin and mass transfer, is part of the gravitational wave plus polarization waveform corresponding to the trajectory in fig. 10.

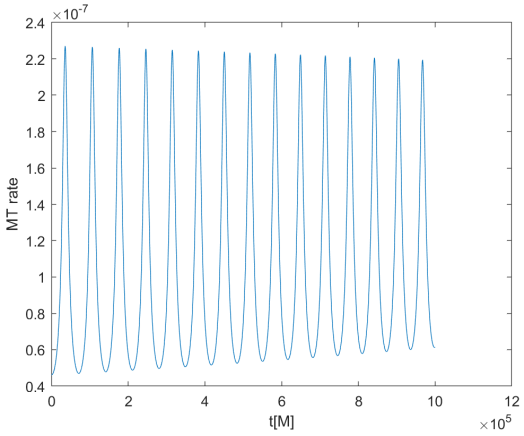

Fig. 10 The above figure displays the evolution of the mass transfer rate (denoted as $\dot{m}_c$) over time for the NS-BH system presented in fig. 10 (with an initial segment extracted). Since our numerical simulation of the orbit starts from the apastron, the spikes in the figure correspond to the periastron. From this, we infer that the mass transfer rate at the periastron has a more significant effect, manifesting as a pronounced amplitude impact on the spikes of the gravitational wave polarization waveform as shown in fig. 9.

spikes in the gravitational wave correspond to motion near the pericenter, where the orbital frequency rapidly increases. According to eq. (89), the mass transfer rate also rapidly increases at the pericenter, causing more matter from the companion star to be accreted there. Consequently, the influence of mass transfer on the orbit is more pronounced at the pericenter, which manifests as a modification in amplitude at the spikes of the waveform. Similar features can also be observed in NS-NS systems[13].

To validate the rationality of our post-Newtonian model, we applied it to a BH-BH system(The initial conditions are shown in table 2.) and compared the results with those obtained from numerical relativity[102]. The outcomes are presented in fig. 11. b

Table 2 The initial parameters of BHBH1360

System	m_1 $(M_\odot)$	m_2 $(M_\odot)$	M $(M_\odot)$	a $(M_\odot^{-1})$	χ_{eff}	q	e
BHBH1360	0.5	0.5	1	16.7	3.25×10^{-9}	1	0.32

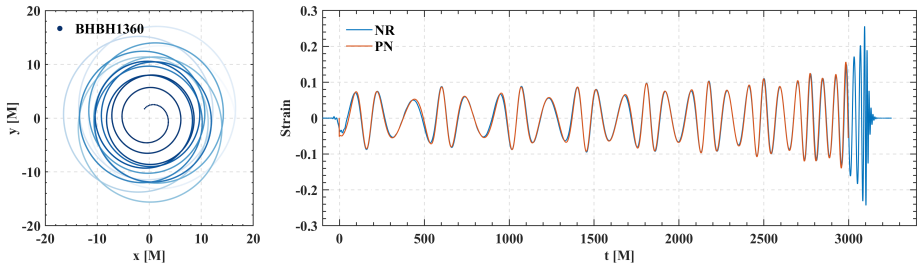

Fig. 11 The above figure presents a comparison between the post-Newtonian and numerical relativity h+ polarized gravitational wave waveform.

The focus of this paper regarding orbital evolution is primarily on gravitational interactions. However, more comprehensive evolutionary mechanisms, such as the precession of spin angular momentum caused by magnetic interactions, changes in orbital energy due to thermonuclear reactions, more detailed processes of stellar winds during mass transfer, including Roche lobe overflow through the L_2/L_3 points, more intricate internal mechanisms of accretion disks, and the continuous influence of luminosity on the accretion rate during the primary star's accretion, among others, can all be investigated within the framework of the model proposed in section 5. In future work, we will employ the model developed here to study more specific astrophysical scenarios.

7 Conclusions

In our research, we recognized that the evolution of compact binary systems exhibits significant relativistic effects, prompting us to adopt a post-Newtonian approach to calculate their evolutionary trajectories. Compact binary systems generally possess spin, and beyond the influence of spin-orbit coupling (primarily driven by tidal forces and electromagnetic interactions leading to dissipation) on orbital evolution in astronomical contexts, spin itself causes spacetime curvature, introducing gravitational effects that modify orbital evolution. Furthermore, real binary systems are not two mass-invariant point masses; mass transfer effects are also a non-negligible factor influencing binary orbital evolution. We found that mass transfer should broadly be discussed in two categories: common envelope evolution and tidal disruption. During common envelope evolution, mass transfer flows are often classified into optically-thin and optically-thick types, which traditionally involve entirely different flow geometries. However, we can establish a unified one-dimensional model based on the Roche potential, assuming that gas primarily flows along the axis connecting the two stars and treating the mass flow as an ideal incompressible gas described by Euler's equations. In this context, isothermal gas as the mass transfer flow can be reduced to the optically-thin scenario, while for general cases, a detailed examination of the equations of states (EOS) is required. Inspired by this, we discovered that a similar mass transfer model

can be constructed for tidal disruption scenarios, where gravity is considered the dominant factor. Thus, the mass transfer rate is derived from the equivalent acceleration (a kind of inertial force) and momentum conservation of an ideal incompressible fluid. From this, we identified three factors influencing the mass transfer rate: the first determined by the binary separation and radial acceleration, the second by the angular velocity and angular acceleration of the binary's orbit, and the third by the outflow rate of the fluid.

We assumed that during mass transfer, matter reaches hydrostatic equilibrium in the direction perpendicular to the orbital plane, ensuring the rationality of our two-dimensional model, and assumed that matter is polytropic in the $yz-plane$. Inspired by methods similar to those used to treat galactic thin accretion disks, we further derived the rate at which matter escapes through the first Lagrange point L_1. Our model assumes that the Roche potential establishes a nozzle-like structure near L_1, similar to a Laval nozzle, revealing that this rate is proportional to the orbital angular velocity. To concurrently address the post-Newtonian correction due to spin and the impact of mass transfer on orbital evolution, we treated the orbit at each moment as a quasi-Keplerian orbit and described orbital evolution within the Keplerian phase space of the orbit. Finally, we employed MATLAB software using the Runge-Kutta method to numerically model the results obtained in this paper, primarily applied to binary systems consisting of neutron stars (NSs) and black holes (BHs)[2]. We numerically find the post-Newtonian effects of NS spin to be negligible (since the density and spin of white dwarfs (WDs) are generally much lower than those of neutron stars, we also deemed their post-Newtonian spin effects negligible). The results indicate that the spin of the black hole can have a non-negligible impact on orbital evolution, while mass transfer accelerates the orbital evolution process, with more pronounced effects near periastron, manifesting as amplitude changes and phase advancements.

More detailed studies require further analysis of the EOS of stars and mass flows, dissipation mechanisms, more complex Roche lobe overflow patterns, energy changes due to thermonuclear reactions, and numerous other finer astrophysical processes, which far exceed the scope of this paper. We will explore these further in future research work.

Acknowledgements. We would like to thank Zihan Zhang and Shuai Zhang from our group for their insightful discussions and valuable suggestions.

References

[1] Einstein, A.: Approximative integration of the field equations of gravitation. Sitzungsber. Preuss. Akad. Wiss. Berlin (Math. Phys.) **1916**(688-696), 1 (1916)

[2] Hulse, R.A., Taylor, J.H.: Discovery of a pulsar in a binary system. Astrophys. J., Lett., v. 195, no. 2, pp. L51-L53 (1975) https://doi.org/10.1086/181708

[2]The Post-Newtonian orbital evolution of compact binary systems containing white dwarfs and the corresponding gravitational waveforms have been thoroughly discussed in another article by our group, see[13].

[3] Mészáros, P., Fox, D.B., Hanna, C., Murase, K.: Multi-messenger astrophysics. Nature Reviews Physics **1**(10), 585–599 (2019)

[4] Abbott, B., Abbott, R., Adhikari, R., Ageev, A., Allen, B., Amin, R., Anderson, S., Anderson, W., Araya, M., Armandula, H., *et al.*: Detector description and performance for the first coincidence observations between ligo and geo. Nuclear Instruments and Methods in Physics Research Section A: Accelerators, Spectrometers, Detectors and Associated Equipment **517**(1-3), 154–179 (2004)

[5] Abbott, B., Abbott, R., Adhikari, R., Ajith, P., Allen, B., Allen, G., Amin, R., Anderson, S., Anderson, W., Arain, M., *et al.*: Ligo: the laser interferometer gravitational-wave observatory. Reports on Progress in physics **72**(7), 076901 (2009)

[6] Acernese, F., Alshourbagy, M., Amico, P., Antonucci, F., Aoudia, S., Arun, K., Astone, P., Avino, S., Baggio, L., Ballardin, G., *et al.*: Virgo status. Classical and Quantum Gravity **25**(18), 184001 (2008)

[7] Mantovani, M.: Virgo and the gravitational interferometry. In: EPJ Web of Conferences, vol. 280, p. 08005 (2023). EDP Sciences

[8] Harry, G.M., LIGO Scientific Collaboration, *et al.*: Advanced ligo: the next generation of gravitational wave detectors. Classical and Quantum Gravity **27**(8), 084006 (2010)

[9] Acernese, F., Agathos, M., Agatsuma, K., Aisa, D., Allemandou, N., Allocca, A., Amarni, J., Astone, P., Balestri, G., Ballardin, G., *et al.*: Advanced virgo: a second-generation interferometric gravitational wave detector. Classical and Quantum Gravity **32**(2), 024001 (2014)

[10] Willke, B., Ajith, P., Allen, B., Aufmuth, P., Aulbert, C., Babak, S., Balasubramanian, R., Barr, B., Berukoff, S., Bunkowski, A., *et al.*: The geo-hf project. Classical and Quantum Gravity **23**(8), 207 (2006)

[11] Punturo, M., Abernathy, M., Acernese, F., Allen, B., Andersson, N., Arun, K., Barone, F., Barr, B., Barsuglia, M., Beker, M., *et al.*: The einstein telescope: A third-generation gravitational wave observatory. Classical and Quantum Gravity **27**(19), 194002 (2010)

[12] Cai, R.-G., Cao, Z., Guo, Z.-K., Wang, S.-J., Yang, T.: The gravitational-wave physics. National Science Review **4**(5), 687–706 (2017)

[13] Zhang, Z.-h., Liu, B., Yu, S.-h., Yang, J.: Gravitational wave forms of galactic compact binaries with mass-transfer correction. Phys. Rev. D **109**(arXiv: 2304.13581) (2024)

[14] Berti, E., Gualtieri, L., Horbatsch, M., Alsing, J.: Light scalar field constraints

from gravitational-wave observations of compact binaries. Physical Review D—Particles, Fields, Gravitation, and Cosmology **85**(12), 122005 (2012)

[15] Zhang, X.-H., Zhao, S.-D., Mohanty, S.D., Liu, Y.-X.: Resolving galactic binaries using a network of space-borne gravitational wave detectors. Physical Review D **106**(10), 102004 (2022)

[16] Blanchet, L.: Post-newtonian theory for gravitational waves. Living Reviews in Relativity **27**(1), 4 (2024)

[17] Blanchet, L., Detweiler, S., Le Tiec, A., Whiting, B.F.: Post-newtonian and numerical calculations of the gravitational self-force for circular orbits in the schwarzschild geometry. Physical Review D—Particles, Fields, Gravitation, and Cosmology **81**(6), 064004 (2010)

[18] Blanchet, L.: Gravitational radiation from post-newtonian sources and inspiralling compact binaries. Living reviews in relativity **17**(1), 2 (2014)

[19] Blanchet, L., Faye, G., Ponsot, B.: Gravitational field and equations of motion of compact binaries to 5/2 post-newtonian order. Physical Review D **58**(12), 124002 (1998)

[20] Damour, T.: The motion of compact bodies and gravitational radiation. In: General Relativity and Gravitation: Invited Papers and Discussion Reports of the 10th International Conference on General Relativity and Gravitation, Padua, July 3–8, 1983, pp. 89–106 (1984). Springer

[21] Bini, D., Damour, T.: Analytical determination of the two-body gravitational interaction potential¡? format?¿ at the fourth post-newtonian approximation. Physical Review D—Particles, Fields, Gravitation, and Cosmology **87**(12), 121501 (2013)

[22] Damour, T., Deruelle, N.: General relativistic celestial mechanics of binary systems (i and ii). Journal des Astronomes Francais **25**, 21 (1985)

[23] Damour, T.: The general relativistic two body problem. arXiv preprint arXiv:1312.3505 (2013)

[24] Jaranowski, P., Schäfer, G.: Third post-newtonian higher order adm hamilton dynamics for two-body point-mass systems. Physical Review D **57**(12), 7274 (1998)

[25] Maggiore, M.: Gravitational Waves: Volume 1: Theory and Experiments. Oxford University Press, ??? (2007). https://doi.org/10.1093/acprof:oso/9780198570745.001.0001 . https://doi.org/10.1093/acprof:oso/9780198570745.001.0001

[26] Wagg, T., Broekgaarden, F.S., Mink, S.E., Frankel, N., Son, L., Justham, S.: Gravitational wave sources in our galactic backyard: Predictions for bhbh, bhns, and nsns binaries detectable with lisa. The Astrophysical Journal **937**(2), 118 (2022)

[27] Tagoshi, H., Ohashi, A., Owen, B.J.: Gravitational field and equations of motion of spinning compact binaries to 2.5 post-newtonian order. Physical Review D **63**(4), 044006 (2001)

[28] Caleb, M., Heywood, I., Rajwade, K., Malenta, M., Willem Stappers, B., Barr, E., Chen, W., Morello, V., Sanidas, S., Van Den Eijnden, J., *et al.*: Discovery of a radio-emitting neutron star with an ultra-long spin period of 76 s. Nature Astronomy **6**(7), 828–836 (2022)

[29] Vahia, M.: Magnetic interaction in binary stars. Astronomy and Astrophysics, v. 300, p. 158 **300**, 158 (1995)

[30] Vasúth, M., Keresztes, Z., Mihály, A., Gergely, L.Á.: Gravitational radiation reaction in compact binary systems: Contribution of the magnetic dipole–magnetic dipole interaction. Physical Review D **68**(12), 124006 (2003)

[31] Most, E.R., Philippov, A.A.: Reconnection-powered fast radio transients from coalescing neutron star binaries. Physical Review Letters **130**(24), 245201 (2023)

[32] Tofflemire, B.M., Mathieu, R.D., Ardila, D.R., Akeson, R.L., Ciardi, D.R., Johns-Krull, C., Herczeg, G.J., Quijano-Vodniza, A.: Accretion and magnetic reconnection in the classical t tauri binary dq tau. The Astrophysical Journal **835**(1), 8 (2017)

[33] Amaro-Seoane, P., Miller, M.C., Kennedy, G.F.: Tidal disruptions of separated binaries in galactic nuclei. Monthly Notices of the Royal Astronomical Society **425**(4), 2401–2406 (2012) https://doi.org/10.1111/j.1365-2966.2012.21162.x https://academic.oup.com/mnras/article-pdf/425/4/2401/4873826/425-4-2401.pdf

[34] Lattimer, J.M., Schramm, D.N.: Tidal disruption of neutron stars by black-holes in close binaries (1976)

[35] Bromley, B.C., Kenyon, S.J., Geller, M.J., Brown, W.R.: Binary disruption by massive black holes: hypervelocity stars, s stars, and tidal disruption events. The Astrophysical Journal Letters **749**(2), 42 (2012)

[36] Thorp, S., Chadwick, E., Sesana, A.: Tidal disruption events from massive black hole binaries: predictions for ongoing and future surveys. Monthly Notices of the Royal Astronomical Society **488**(3), 4042–4060 (2019)

[37] Savonije, G.: Roche-lobe overflow and massive x-ray binary systems. Astronomy and Astrophysics, vol. 71, no. 3, Jan. 1979, p. 352-358. **71**, 352–358 (1979)

[38] Mohamed, S., Podsiadlowski, P.: Wind roche-lobe overflow: a new mass-transfer mode for wide binaries. In: 15th European Workshop on White Dwarfs, vol. 372, p. 397 (2007)

[39] Reichardt, T.A., De Marco, O., Iaconi, R., Tout, C.A., Price, D.J.: Extending common envelope simulations from roche lobe overflow to the nebular phase. Monthly Notices of the Royal Astronomical Society **484**(1), 631–647 (2019)

[40] Ivanova, N., Justham, S., Ricker, P.: Common Envelope Evolution. IOP Publishing, ??? (2020)

[41] Taam, R.E., Sandquist, E.L.: Common envelope evolution of massive binary stars. Annual Review of Astronomy and Astrophysics **38**(1), 113–141 (2000)

[42] Chamandy, L., Frank, A., Blackman, E.G., Carroll-Nellenback, J., Liu, B., Tu, Y., Nordhaus, J., Chen, Z., Peng, B.: Accretion in common envelope evolution. Monthly Notices of the Royal Astronomical Society **480**(2), 1898–1911 (2018)

[43] Theuns, T., Boffin, H.M., Jorissen, A.: Wind accretion in binary stars—ii. accretion rates. Monthly Notices of the Royal Astronomical Society **280**(4), 1264–1276 (1996)

[44] Ivanov, P., Papaloizou, J., Polnarev, A.: The evolution of a supermassive binary caused by an accretion disc. Monthly Notices of the Royal Astronomical Society **307**(1), 79–90 (1999)

[45] Vanbeveren, D.: The influence of the radiation pressure force on possible critical surfaces in binary systems. Astrophysics and Space Science **57**, 41–51 (1978)

[46] Zhou, H.-N., Leung, K.-C.: The influence of radiation pressure on equipotential surfaces in high-temperature binary systems. Astrophysics and space science **141**, 257–270 (1988)

[47] Hillebrandt, W., Niemeyer, J.C.: Type ia supernova explosion models. Annual Review of Astronomy and Astrophysics **38**(1), 191–230 (2000)

[48] Liu, Z.-W., Röpke, F.K., Han, Z.: Type ia supernova explosions in binary systems: A review. Research in Astronomy and Astrophysics **23**(8), 082001 (2023)

[49] Wheeler, J.C., Lecar, M., McKee, C.F.: Supernovae in binary systems. Astrophysical Journal, vol. 200, Aug. 15, 1975, pt. 1, p. 145-157. **200**, 145–157 (1975)

[50] Wheeler, J.C., Hansen, C.J.: Thermonuclear detonations in collapsing white

dwarf stars. Astrophysics and Space Science **11**(3), 373–397 (1971)

[51] Tauris, T.M., Heuvel, E.P.: Physics of Binary Star Evolution: From Stars to X-ray Binaries and Gravitational Wave Sources vol. 42. Princeton University Press, ??? (2023)

[52] Cehula, J., Pejcha, O.: A theory of mass transfer in binary stars. Monthly Notices of the Royal Astronomical Society **524**(1), 471–490 (2023)

[53] Asano, K.: Mass Transfer: from Fundamentals to Modern Industrial Applications. John Wiley & Sons, ??? (2007)

[54] Dosopoulou, F., Kalogera, V.: Orbital evolution of mass-transferring eccentric binary systems. i. phase-dependent evolution. The Astrophysical Journal **825**(1), 70 (2016)

[55] Dosopoulou, F., Kalogera, V.: Orbital evolution of mass-transferring eccentric binary systems. ii. secular evolution. The Astrophysical Journal **825**(1), 71 (2016)

[56] Yu, S., Lu, Y., Jeffery, C.S.: Orbital evolution of neutron-star–white-dwarf binaries by roche lobe overflow and gravitational wave radiation. Monthly Notices of the Royal Astronomical Society **503**(2), 2776–2790 (2021)

[57] Gallegos-Garcia, M., Berry, C.P., Kalogera, V.: Evolutionary origins of binary neutron star mergers: Effects of common envelope efficiency and metallicity. The Astrophysical Journal **955**(2), 133 (2023)

[58] Okazaki, A.T., Hayasaki, K., Moritani, Y.: Origin of two types of x-ray outbursts in be/x-ray binaries. i. accretion scenarios. Publications of the Astronomical Society of Japan **65**(2), 41 (2013)

[59] Shakura, N.I., Sunyaev, R.A.: Black holes in binary systems. observational appearance. Astronomy and Astrophysics, Vol. 24, p. 337-355 **24**, 337–355 (1973)

[60] Balbus, S.A., Hawley, J.F.: A powerful local shear instability in weakly magnetized disks. i-linear analysis. ii-nonlinear evolution. Astrophysical Journal, Part 1 (ISSN 0004-637X), vol. 376, July 20, 1991, p. 214-233. **376**, 214–233 (1991)

[61] King, A.R., Pringle, J., Livio, M.: Accretion disc viscosity: how big is alpha? Monthly Notices of the Royal Astronomical Society **376**(4), 1740–1746 (2007)

[62] Heinzeller, D., Duschl, W.: On the eddington limit in accretion discs. Monthly Notices of the Royal Astronomical Society **374**(3), 1146–1154 (2007)

[63] Crawford, J.: On the subgiant components of eclipsing binary systems. Astrophysical Journal, vol. 121, p. 71 **121**, 71 (1955)

[64] Morton, D.C.: Evolutionary mass exchange in close binary systems. Astrophysical Journal, vol. 132, p. 146 **132**, 146 (1960)

[65] Pustylnik, I.: The early history of resolving the algol paradox. Astronomical and Astrophysical Transactions **15**(1-4), 357–362 (1998)

[66] Hayakawa, S., Matsuoka, M.: Part v. origin of cosmic x-rays. Progress of Theoretical Physics Supplement **30**, 204–228 (1964)

[67] Zeldovich, Y.B., Guseynov, O.: Collapsed stars in binaries. Astrophysical Journal, vol. 144, p. 840 **144**, 840 (1966)

[68] Pringle, J., Rees, M.: Accretion disc models for compact x-ray sources. Astronomy and Astrophysics, Vol. 21, p. 1 (1972) **21**, 1 (1972)

[69] Boyle, C.B.: Mass transfer and accretion in close binaries: A review. Vistas in astronomy **27**, 149–169 (1984)

[70] Schatzman, E.: Remarques sur le phénomàne de nova (viii). Annales d'Astrophysique, Vol. 21, p. 1 **21**, 1 (1958)

[71] Kraft, R.P.: Binary stars among cataclysmic variables iii: Ten old novae. In: A Source Book in Astronomy and Astrophysics, 1900–1975, pp. 421–429. Harvard University Press, ??? (1979)

[72] Fan, Y.-Z., Lai, X.-B., Dong, Y.-Q., Liu, Y.-X.: Polarization modes of gravitational waves in scalar-tensor-rastall theory. The European Physical Journal C **85**(1), 1–14 (2025)

[73] Figueroa, D.G., Garcia-Bellido, J., Rajantie, A.: On the transverse-traceless projection in lattice simulations of gravitational wave production. Journal of Cosmology and Astroparticle Physics **2011**(11), 015 (2011)

[74] Blanchet, L., Faye, G.: Hadamard regularization. Journal of Mathematical Physics **41**(11), 7675–7714 (2000)

[75] Sellier, A.: Hadamard's finite part concept in dimension $n \geq 2$, distributional definition, regularization forms and distributional derivatives. Proceedings of the Royal Society of London. Series A: Mathematical and Physical Sciences **445**(1923), 69–98 (1994)

[76] Papapetrou, A.: Spinning test-particles in general relativity. i. Proceedings of the Royal Society of London. Series A. Mathematical and Physical Sciences **209**(1097), 248–258 (1951)

[77] Barker, B.M., O'Connell, R.F.: The gravitational interaction: Spin, rotation, and quantum effects-a review. General Relativity and Gravitation **11**, 149–175 (1979)

[78] Kidder, L.E., Will, C.M., Wiseman, A.G.: Spin effects in the inspiral of coalescing compact binaries. Physical Review D **47**(10), 4183 (1993)

[79] Kidder, L.E.: Coalescing binary systems of compact objects to (post) 5/2-newtonian order. v. spin effects. Physical Review D **52**(2), 821 (1995)

[80] HOJMAN, S.A.: Electromagnetic and Gravitational Interactions of a Relativistic Spherical Top. Princeton University, ??? (1975)

[81] Lu, W., Fuller, J., Quataert, E., Bonnerot, C.: On rapid binary mass transfer–i. physical model. Monthly Notices of the Royal Astronomical Society **519**(1), 1409–1424 (2023)

[82] Kolb, U., Ritter, H.: A comparative study of the evolution of a close binary using a standard and an improved technique for computing mass transfer. Astronomy and Astrophysics (ISSN 0004-6361), vol. 236, no. 2, Sept. 1990, p. 385-392. **236**, 385–392 (1990)

[83] Bath, G., Pringle, J.: The evolution of viscous discs–i. mass transfer variations. Monthly Notices of the Royal Astronomical Society **194**(4), 967–986 (1981)

[84] Raptis, A.: Free convective oscillatory flow and mass transfer past a porous plate in the presence of radiation for an optically thin fluid. Thermal Science **15**(3), 849–857 (2011)

[85] Tylenda, R.: Radiation from optically thin accretion discs. Acta Astronomica, Vol. 31, P. 127, 1981 **31**, 127 (1981)

[86] Ritter, H.: Turning on and off mass transfer in cataclysmic binaries. Astronomy and Astrophysics (ISSN 0004-6361), vol. 202, no. 1-2, Aug. 1988, p. 93-100. **202**, 93–100 (1988)

[87] Jackson, B., Arras, P., Penev, K., Peacock, S., Marchant, P.: A new model of roche lobe overflow for short-period gaseous planets and binary stars. The Astrophysical Journal **835**(2), 145 (2017)

[88] Margalit, B., Metzger, B.D.: Time-dependent models of accretion discs with nuclear burning following the tidal disruption of a white dwarf by a neutron star. Monthly Notices of the Royal Astronomical Society **461**(2), 1154–1176 (2016) https://doi.org/10.1093/mnras/stw1410 https://academic.oup.com/mnras/article-pdf/461/2/1154/8107721/stw1410.pdf

[89] Lubow, S.H., Shu, F.H.: Gas dynamics of semidetached binaries. Astrophysical Journal, vol. 198, June 1, 1975, pt. 1, p. 383-405. **198**, 383–405 (1975)

[90] Verbunt, F., Rappaport, S.: Mass transfer instabilities due to angular momentum

flows in close binaries. Astrophysical Journal, Part 1 (ISSN 0004-637X), vol. 332, Sept. 1, 1988, p. 193-198. **332**, 193–198 (1988)

[91] Kudoh, T., Matsumoto, R., Shibata, K.: Effect of a magneto-rotational instability on jets from accretion disks. Publications of the Astronomical Society of Japan **54**(1), 121–130 (2002)

[92] Balbus, S.A., Hawley, J.F.: A powerful local shear instability in weakly magnetized disks: I. linear analysis. In: Bulletin of the American Astronomical Society, Vol. 22, P. 1209, vol. 22, p. 1209 (1990)

[93] Nixon, C.: Accretion disc viscosity: a limit on the anisotropy. Monthly Notices of the Royal Astronomical Society **450**(3), 2459–2465 (2015) https://doi.org/10.1093/mnras/stv796 https://academic.oup.com/mnras/article-pdf/450/3/2459/18509316/stv796.pdf

[94] Kley, W., Papaloizou, J.: Causal viscosity in accretion disc boundary layers. Monthly Notices of the Royal Astronomical Society **285**(2), 239–252 (1997)

[95] Ruderman, M.A., Shaham, J.: Fate of very low-mass secondaries in accreting binaries and the 1.5-ms pulsar. Nature **304**(5925), 425–427 (1983)

[96] Campbell, C.: Magnetic coupling in am herculis binaries. Monthly Notices of the Royal Astronomical Society **205**(4), 1031–1052 (1983)

[97] Campbell, C.: Tidal effects in twin-degenerate binaries. Monthly Notices of the Royal Astronomical Society **207**(3), 433–443 (1984)

[98] Pavlovskii, K., Ivanova, N.: Mass transfer from giant donors. Monthly Notices of the Royal Astronomical Society **449**(4), 4415–4427 (2015)

[99] Piro, A.L.: Magnetic interactions in coalescing neutron star binaries. The Astrophysical Journal **755**(1), 80 (2012)

[100] Ioka, K., Taniguchi, K.: Gravitational waves from inspiraling compact binaries with magnetic dipole moments. The Astrophysical Journal **537**(1), 327 (2000)

[101] Zweibel, E.G., Yamada, M.: Magnetic reconnection in astrophysical and laboratory plasmas. Annual review of astronomy and astrophysics **47**(1), 291–332 (2009)

[102] Boyle, M., Hemberger, D., Iozzo, D.A., Lovelace, G., Ossokine, S., Pfeiffer, H.P., Scheel, M.A., Stein, L.C., Woodford, C.J., Zimmerman, A.B., *et al.*: The sxs collaboration catalog of binary black hole simulations. Classical and Quantum Gravity **36**(19), 195006 (2019)